国内学会

1. 石井輝、今牧博貴、森　潔、栗原孝成、笠原正登、横井秀基、古賀健一、森慶太、加藤有希子、戸田尚宏、大野祥子、菅原照、柳田素子、中尾一和、向山政志
分泌シグナル Ngal による肥満の positive feedback
第 87 回日本内分泌学会学術総会 2014 年 4 月 24-26 日 福岡

2. 大野祥子、横井秀基、笠原正登、森　潔、桑原宏一郎、藤倉純二、内藤雅喜、栗原孝成、今牧博貴、石井輝、古賀健一、沼田朋大、菅原照、森泰生、柳田素子、中尾一和、向山政志
糖尿病性腎症における N 型 Ca2+チャネル阻害の意義
第 57 回日本糖尿病学会年次学術集会 2014 年 5 月 22-24　大阪

3. 石井輝、今牧博貴、栗原孝成、笠原正登、横井秀基、古賀健一、森慶太、加藤有希子、戸田尚宏、大野祥子、菅原照、柳田素子、中尾一和、向山政志、森　潔
分泌シグナル Ngal の糖脂質代謝における意義
第 57 回日本糖尿病学会年次学術集会 2014 年 5 月 24 日　大阪

4. 加藤有希子、横井秀基、森　潔、笠原正登、小川喜久、栗原孝成、徳留　健、岸本一郎、菅原照、中尾一和、柳田素子、向山政志
アルドステロンによるポドサイト傷害に対するナトリウム利尿ペプチドＡ受容体の機能解析
第 57 回日本腎臓学会学術総会 2014 年 7 月 6 日　横浜

5. 森慶太、森　潔、笠原正登、横井秀基、栗原孝成、今牧博貴、石井輝、戸田尚宏、中尾一和、柳田素子、向山政志
糸球体および近位尿細管に全く障害がないモデルにおける蛋白再吸収阻害の影響
第 57 回日本腎臓学会学術総会 2014 年 7 月 6 日　横浜

6. 古賀健一、横井秀基、森　潔、笠原正登、栗原孝成、今牧博貴、菅原照、中尾一和、柳田素子、向山政志
TGF-β/CTGF/Smad シグナルを調節する microRNA-26a の糖尿病性腎症糸球体おける発現解析
第 57 回日本腎臓学会学術総会 2014 年 7 月 4 日　横浜

7. 今牧博貴、森　潔、森慶太、石井　輝、栗原孝成、笠原正登、横井秀基、古賀健一、加藤有希子、戸田尚宏、大野祥子、中尾一和、柳田素子、向山政志
健常人及び腎不全症例における血中・尿中 NGAL の分子量の違い
第 57 回日本腎臓学会学術総会 2014 年 7 月 4 日　横浜

8. 加藤有希子、横井秀基、森　潔、笠原正登、小川喜久、栗原孝成、徳留健、岸本一郎、菅原 照、中尾一和、柳田素子、向山政志
アルドステロンによるポドサイト傷害に対する Na 利尿ペプチド/GC-A 系の保護作用の検討
第 37 回日本高血圧学会総会 2014 年 10 月 19 日　横浜

9. 石井輝、笠原正登、横井秀基、栗原孝成、保野慎治、森　潔、藤本 明、田中佐智子、浅原哲子、阪本 貴、森井成人、堀井和子、酒井 建、向山政志、上嶋健治
アムロジピン内服下の高血圧患者の圧利尿曲線に及ぼすアトルバスタチンの影響(DUET 試験)
第 37 回日本高血圧学会総会 2014 年 10 月 19 日　横浜

10. 小口綾貴子、横井秀基、今牧博貴、栗原孝成、清水葉子、笠原正登、向山政志、塚本達雄、柳田素子
腹膜透析中に急激に心嚢水・胸水を発症し血液透析移行後著名に改善した心外膜炎の一例
第 20 回日本腹膜透析医学会学術集会 2014 年 9 月 6 日　山形

H. 知的財産権の出願・登録状況

なし

厚生労働科学研究費補助金（創薬基盤推進研究事業）
分担研究報告書

新規創薬を目指した生活習慣病・難治性疾患モデル遺伝子変異ラットの開発と解析
－糖尿病・メタボリックシンドロームモデル遺伝子変異ラット糖代謝・膵内分泌機能解析-

分担研究者：富田　努　　京都大学大学院医学研究科　糖尿病内分泌栄養内科
特定病院助教

研究要旨　　本研究課題は、新規開発した標的遺伝子変異ラット開発システムを用いて、生活習慣病や難治性疾患に関連する複数の遺伝子変異ラットを開発し、新規生活習慣病・難治性疾患モデルラットを樹立し、従来マウスにおいて実施・解析が困難であった系統的な生理学的解析、移植実験、薬理薬効評価解析などの施行を容易にする事により、生活習慣病関連疾患、難治性疾患の病態解明、新規治療標的の同定および創薬開発を加速させることを目的とする。本年度は、糖尿病、メタボリックシンドロームに関連した生活習慣病・難治性疾患関連遺伝子変異ラットのスクリーニングの過程で同定し系統樹立した、レプチンおよびSeipin遺伝子変異ラットの系統樹立の糖代謝、膵内分泌機能に関する解析を前年度より継続して行い、GPR40 やPdx1遺伝子発現低下を認めた。今後も、樹立した遺伝子変異ラットの表現系解析を行い、病態解明研究を行うとともに、新規創薬開発への応用を探る。

A. 研究目的

現在生活習慣病関連疾患である心筋梗塞、心不全、糖尿病、脳卒中、慢性腎臓病(CKD)などの病態解明、新規治療標的同定に基づく新規治療薬、治療法開発が望まれている。現在これら疾患の病態解析、創薬開発、再生医療研究には遺伝子改変技術が確立されているマウスがモデル動物として多く用いられているが、マウスはその小ささゆえに採血や組織採取(膵臓、中枢神経系)が困難であること、生理学的解析や移植実験が行ないにくいなどの問題がある。さらに、最近では代謝面においてヒトと大きく異なる生理的特徴が明らかとなった(Vassilopoulos, et al.Science 2009)。そのため、マウスと比べ体のサイズが大きく、採血や組織採取や系統的な生理学的解析が容易で、移植実験も行ないやすく、代謝面でもよりヒトに近いラットでの疾患モデル確立が期待されている。しかし、現時点ではES細胞の技術がラットで未確立のため、遺伝子改変ラットの効率的な作成は不可能である。最近京都大学　動物実験施設の芹川、真下らはENUミュータジェネシスに、新規DNAスクリーニング法(MuT-power)、凍結精子アーカイブからの個体復元技術(ICSI)という一連の新規技術を組み合わせることにより、標的遺伝子変異ラットの効率的な作成システム構築に成功した。本研究課題では、このシステムを用いて生活習慣病関連・難治性疾患遺伝子変異ラットをスクリーニングし、その表現系を解析することにより糖尿病、メタボリックシンドロームなどの新規生活習慣病モデルラットを開発し、その詳細な解析を通して病態解明、新規治療標的同定を行なうと共に、このモデルを用いた新規創薬開発を加速させることを目的とする。

B. 研究方法

生活習慣病・難治性疾患関連遺伝子に関するENUミュータジェネシスによる約1600匹分のラットミュータントアーカイブの高速DNAスクリーニングを行い、糖尿病、メタボリックシンドローム関連遺伝子変異として、レプチンおよびseipin遺伝子の変異ラットの同定を行い、その系統樹立に成功した。本年度は特にこれら変異ラットの糖代謝、膵内分泌機能に関して解析をおこなった。これら実験動物を用いる研究に際しては「動物の愛護および管理に関する法律」（平成１７年６月改正法）、「京都大学における動物実験の実施に関する規程」および「京都大学大学院医学研究科・医学部における動物実験の実施に関する規程」（いずれも平成１９年４月改訂）を遵守して実施し、動物に与える苦痛を最小限にとどめるように最善の配慮を尽くしている。

C. 研究結果

生活習慣病・難治性疾患関連遺伝子に関するENUミュータジェネシスによる約1600匹分のラットミュータントアーカイブの高速DNAスクリーニングの結果レプチンおよびseipin、遺伝子に変異を有するラットの同定に成功し、さらに独自開発した個体復元技術ICSIを用いて標的遺伝子変異ラット系統樹立に成功し、表現系解析を行った。その結果、レプチン遺伝子ナンセンス変異ラットでは明らかな肥満と摂食量の亢進をみとめた。レプチン遺伝子ナンセンス変異ラットに糖負荷試験を行った結果、血中グルコース濃度高値、高インスリン血症を認め、耐糖能の異常、インスリン抵抗性の存在が確認された。また、中性脂肪高値、遊離脂肪酸高値、総コレステロール値高値などの脂質異常も見出された。また、レプチン遺伝子ナンセンス変異ラットの膵臓では、ラ氏島の拡大を認め、beta細胞などの肥大が考えられた。本変異ラットの膵頭におけるGPR40、Pdx1の遺伝子発現を検討したところ、いずれも約50%に低下していた。このことから本レプチン遺伝子変異ラットの食後高血糖、インスリン初期分泌低下にこれら遺伝子産物の発現低下が関与する可能性が示唆された。一方、脂肪委縮症の原因遺伝子であるseipin遺伝子の変異ラットの解析も昨年に引き続き行った。今後、更に詳細な解析を継続していく予定である。

D. 考察

生活習慣病関連疾患の病態解明においては複数の臓器における病態の同時進行的変化とそれに伴う液性因子を介した臓器間シグナルクロストーク解明が必須であり、またこれら病態には細胞老化も関与するため、その治療において細胞・臓器再生という観点も不可欠である。現在これら疾患の病態解析、創薬開発、再生医療研究には遺伝子改変技術が確立されているマウスがモデル動物として多く用いられているが、マウスはその小ささゆえに採血や組織採取が困難であること、生理学的解析や移植実験が行ないにくいなどの問題がある。そのため、マウスと比べ体のサイズが大きく、採血や組織採取や系統的な生理学的解析が容易で、移植実験も行ないやすく、代謝面でもよりヒトに近いラットでの疾患モデル確立が期待されている。実際今回得られたレプチンおよびseipin遺伝子変異ラットにおいて代謝パラメーターの解析においてより安定した結果を得られること、また、膵組織の詳細な組織学的解析および分子生物学的解析が可能であることが確認された。今後その表現系を、さらに詳細に解析することにより、これら遺伝子変異ラットのモデル動物としての意義が確立されれば、病態解明・新規治療標的同定および新規創薬開発への応用を進めていきたい。

E. 結論

生活習慣病・難治性疾患関連遺伝子に関して、複数の糖尿病、メタボリックシンドローム関連遺伝子変異ラットの同定、系統樹立に成功し、本年度はその中でレプチンおよびseipin遺伝子変異ラットの表現系、特に糖脂質代謝および膵島の遺伝子発現の解析を前年度の引き続き行った。今後これら遺伝子変異ラットの表現系解析をさらに継続し、疾患モデルラットとしての意義を確立し、病態解明・新規治療標的同定と新規創薬開発への応用を進めていきたい。

F. 健康危険情報

なし

G. 研究発表

1. 論文発表

1. Tomita T, Hosoda K, Fujikura J, Inagaki N, Nakao K.
   The G-Protein-Coupled Long-Chain Fatty Acid Receptor GPR40 and Glucose Metabolism.
   Front Endocrinol (Lausanne). 2014. 5:152.

2. 学会発表

国内学会

1. 吉良友里、冨田努、細田公則、藤倉純二、海老原千尋、阿部恵、海老原健、中尾一和、稲垣暢也
   新規の遺伝性肥満モデル *mkyo/mkyo*

ラット膵島における脂質受容体GPR40の遺伝子発現調節
第 88 回日本内分泌学会学術総会、2015.4.23-25、仙台国際センター

2. 吉良友里、冨田努、細田公則、藤倉純二、海老原千尋、阿部　恵、海老原健、中尾一和、稲垣暢也
新規の遺伝性肥満モデル *mkyo/mkyo* ラット膵島における脂質受容体GPR40の遺伝子発現調節
第 58 回日本糖尿病学会年次学術集会、2015.5.21-24、山口県下関市

H. 知的財産権の出願・登録状況
なし

研究成果の刊行に関する一覧表

雑誌

発表者氏名	論文タイトル名	発表誌名	巻号	ページ	出版年
Sakai T, Kusakabe T, Ebihara K, Aotani D, Yamamoto-Kataoka S, Zhao M, Gumbilai VM, Ebihara C, Aizawa-Abe M, Yamamoto Y, Noguchi M, Fujikura J, Hosoda K, Inagaki N, Nakao K	Leptin restores the insulinotropic effect of exenatide in a mouse model of type 2 diabetes with increased adiposity induced by streptozotocin and high-fat diet.	**Am J Physiol Endocrinol Metab**	307	E712-719	2014
Tanaka M, Yamaguchi S, Yamazaki Y, Kinoshita H, Kuwahara K, Nakao K, Jay PY, Noda T, Nakamura T.	Somatic chromosomal translocation between *Ewsr1* and *Fli1* loci leads to dilated cardiomyopathy in a mouse model	**Sci Rep**	5	7826	2015
Oshita K, Itoh M, Hirashima S, Kuwabara Y, Ishihara K, Kuwahara K, Nakao K, Kimura T, Nakamura K, Ushijima K, Takano M.	Ectopic automaticity induced in ventricular myocytes by transgenic overexpression of HCN2	**J Mol Cell Cardiol**	80	81-89	2015
Yamada Y, Kinoshita H, Kuwahara K, Nakagawa Y, Kuwabara Y, Minami T, Yamada C, Shibata J, Nakao K, Cho K, Arai Y, Yasuno S, Nishikimi T, Ueshima K, Kamakura S, Nishida M, Kiyonaka S, Mori Y, Kimura T, Kangawa K, Nakao K	Inhibition of N-type Ca^{2+} channels ameliorates an imbalance in cardiac autonomic nerve activity and prevents lethal arrhythmias in mice with heart failure	**Cardiovascular Research**	104	1. 183-93	2014
Nakagawa Y, Nishikimi T, Kuwahara K, Yasuno S, Kinoshita H, Kuwabara Y, Nakao K, Minami T, Yamada C, Ueshima K, Ikeda Y, Okamoto H, Horii K, Nagata K, Kangawa K, Minamino N, Nakao K.	The Effects of Super-Flux (High Performance) Dialyzer on Plasma Glycosylated Pro-B-Type Natriuretic Peptide (proBNP) and Glycosylated N-Terminal proBNP in End-Stage Renal Disease Patients on Dialysis	**PLoS One**	9	e92314	2014
Kuwabara T, Mori K, Mukoyama M, Kasahara M, Yokoi H, Nakao K	Macrophage-mediated glucolipotoxicity via myeloid-related protein 8/toll-like receptor 4 signaling in diabetic nephropathy	**Clin Exp Nephrol**	18	584-592	2014

Kuwabara T, Mori K, Kasahara M, Yokoi H, Imamaki H, Ishii A, Koga K, Sugawara A, Yasuno S, Ueshima K, Morikawa T, Konishi Y, Imanishi M, Nishiyama A, Naka o K, Mukoyama M.	Predictive significance of kidney myeloid-related protein 8 expression in patients with obesity- or type 2 diabetes-associated kidney diseases.	**PLoS One**	9	e88942	2014
Kanda J, Mori K, Kawabata H, Kuwabara T, Mori KP, I mamaki H, Kasahara M, Yokoi H, Mizumoto C, Thoennis sen NH, Koeffler HP, Barasch J, Takaori-Kondo A, Muko yama M, Nakao K.	An AKI biomarker lipocalin 2 in the blood derives from the kidney in renal injury but from neutrophils in normal and infected conditions.	**Clin Exp Nephrol**	19	99-106	2015
Tomita T, Hosoda K, Fujikura J, Inagaki N, Nakao K.	The G-Protein-Coupled Long-Chain Fatty Acid Receptor GPR40 and Glucose Metabolism.	**Front Endocrinol**	5	152	2014
Ebihara C, Ebihara K, Aizawa-Abe M, Mashimo T, Tomit a T, Zhao M, Gumbilai V, Kusakabe T, Yamamoto Y, A otani D, Yamamoto-Kataoka S, Sakai T, Hosoda K, Serik awa T, Nakao K.	Seipin is necessary for normal brain development and spermatogenesis in addition to adipogenesis.	**Hum Mol Genet**		In press	2015

Am J Physiol Endocrinol Metab 307: E712–E719, 2014.
First published August 26, 2014; doi:10.1152/ajpendo.00272.2014.

Leptin restores the insulinotropic effect of exenatide in a mouse model of type 2 diabetes with increased adiposity induced by streptozotocin and high-fat diet

Takeru Sakai,[1,2] Toru Kusakabe,[2] Ken Ebihara,[3] Daisuke Aotani,[2] Sachiko Yamamoto-Kataoka,[1] Mingming Zhao,[1] Valentino Milton Junior Gumbilai,[1] Chihiro Ebihara,[1] Megumi Aizawa-Abe,[3] Yuji Yamamoto,[1] Michio Noguchi,[2] Junji Fujikura,[1] Kiminori Hosoda,[2,4] Nobuya Inagaki,[1] and Kazuwa Nakao[2]

[1]*Department of Diabetes, Endocrinology, and Nutrition, Kyoto University Graduate School of Medicine, Kyoto, Japan;* [2]*Medical Innovation Center, Kyoto University Graduate School of Medicine, Kyoto, Japan;* [3]*Institute for Advancement of Clinical and Translational Science, Kyoto University Hospital, Kyoto, Japan; and* [4]*Department of Human Health Science, Kyoto University Graduate School of Medicine, Kyoto, Japan*

Submitted 11 June 2014; accepted in final form 25 August 2014

Sakai T, Kusakabe T, Ebihara K, Aotani D, Yamamoto-Kataoka S, Zhao M, Gumbilai VM, Ebihara C, Aizawa-Abe M, Yamamoto Y, Noguchi M, Fujikura J, Hosoda K, Inagaki N, Nakao K. Leptin restores the insulinotropic effect of exenatide in a mouse model of type 2 diabetes with increased adiposity induced by streptozotocin and high-fat diet. *Am J Physiol Endocrinol Metab* 307: E712–E719, 2014. First published August 26, 2014; doi:10.1152/ajpendo.00272.2014.—Leptin may reduce pancreatic lipid deposition, which increases with progression of obesity and can impair β-cell function. The insulinotropic effect of glucagon-like peptide-1 (GLP-1) and the efficacy of GLP-1 receptor agonist are reduced associated with impaired β-cell function. In this study, we examined whether leptin could restore the efficacy of exenatide, a GLP-1 receptor agonist, in type 2 diabetes with increased adiposity. We chronically administered leptin (500 $\mu g \cdot kg^{-1} \cdot day^{-1}$) and/or exenatide (20 $\mu g \cdot kg^{-1} \cdot day^{-1}$) for 2 wk in a mouse model of type 2 diabetes with increased adiposity induced by streptozotocin and high-fat diet (STZ/HFD mice). The STZ/HFD mice exhibited hyperglycemia, overweight, increased pancreatic triglyceride level, and reduced glucose-stimulated insulin secretion (GSIS); moreover, the insulinotropic effect of exenatide was reduced. However, leptin significantly reduced pancreatic triglyceride level, and adding leptin to exenatide (LEP/EX) remarkably enhanced GSIS. These results suggested that the leptin treatment restored the insulinotropic effect of exenatide in the mice. In addition, LEP/EX reduced food intake, body weight, and triglyceride levels in the skeletal muscle and liver, and corrected hyperglycemia to a greater extent than either monotherapy. The pair-feeding experiment indicated that the marked reduction of pancreatic triglyceride level and enhancement of GSIS by LEP/EX occurred via mechanisms other than calorie restriction. These results suggest that leptin treatment may restore the insulinotropic effect of exenatide associated with the reduction of pancreatic lipid deposition in type 2 diabetes with increased adiposity. Combination therapy with leptin and exenatide could be an effective treatment for patients with type 2 diabetes with increased adiposity.

drug therapy; combination; insulin secretion

LEPTIN, AN ADIPOCYTE-DERIVED hormone, has therapeutic potential for treating diabetes and obesity (7, 13 19, 27, 32, 34). In our previous clinical trial in patients with lipodystrophy (6), we confirmed the therapeutic usefulness of leptin as a glucose-lowering agent, and it was first approved for the treatment of lipodystrophy in Japan in March 2013. Given these glucoregulatory effects of leptin, we and others have reported the therapeutic usefulness of leptin for various forms of diabetes, including type 2 diabetes, in rodent models (20, 23, 26, 28, 47). The glucoregulatory effects of leptin are associated with the reduction of ectopic lipid deposition, which increases with progression of obesity (36, 39, 46). The reduction of ectopic lipid deposition in the liver and skeletal muscle could improve insulin sensitivity (42). In the pancreas, the reduction of ectopic lipid deposition could improve β-cell function such as glucose-stimulated insulin secretion (GSIS) in rodents and humans (22, 39, 46).

On the other hand, glucagon-like peptide-1 (GLP-1), a hormone released from the L cells of the intestine, improves glucose metabolism by enhancing GSIS (18). However, in patients with type 2 diabetes, the insulinotropic effect of GLP-1 is substantially reduced (15, 29). This reduction may be a consequence of the diabetic state rather than a contributor to it (30). Chronic hyperglycemia and hyperlipidemia could reduce β-cell function and could reduce the insulinotropic effect of GLP-1 (10, 15). The correction of both these abnormalities may restore β-cell function and may restore the insulinotropic effects of GLP-1 (11, 14, 49). Pancreatic lipid deposition can also reduce β-cell function (41, 45), but its effect on the insulinotropic effect of GLP-1 remains unknown.

In patients with type 2 diabetes, pancreatic lipid deposition increases with progression of obesity, and GSIS is reduced (17, 36, 41, 45). Therefore, we speculated that leptin could restore the insulinotropic effect of GLP-1 associated with the reduction of pancreatic lipid deposition and enhance the efficacy of GLP-1 receptor agonists. If this hypothesis is confirmed, we might be able to manage type 2 diabetes more effectively.

In the present study, we examined whether leptin could reduce pancreatic lipid deposition and enhance the insulinotropic effect of exenatide, a GLP-1 receptor agonist, in a mouse model of type 2 diabetes with increased adiposity induced by streptozotocin (STZ) and high-fat diet (HFD) (STZ/HFD mice) (20).

MATERIALS AND METHODS

Animals. Seven-week old male C57BL/6J mice were purchased from Japan SLC (Shizuoka, Japan). The mice were individually caged and kept at a constant room temperature (25°C) under a 12:12-h light-dark cycle with ad libitum access to water and a standard diet

Address for reprint requests and other correspondence: T. Kusakabe; Medical Innovation Center, Kyoto Univ. Graduate School of Medicine, 53 Shogoin-Kawahara-cho, Sakyo-ku, Kyoto 606-8507, Japan (e-mail: kusakabe@kuhp.kyoto-u.ac.jp).

(SD; NMF, 3.5 kcal/g, and 13% of energy as fat; Oriental Yeast, Tokyo, Japan). Animal care and all experiments were conducted in accordance with the Guidelines for Animal Experiments of Kyoto University and were approved by the Animal Research Committee, Graduate School of Medicine, Kyoto University.

Generation of the mouse model of type 2 diabetes with increased adiposity. We generated a mouse model of type 2 diabetes with increased adiposity, as described previously (20). Eight-week-old male C57BL/6J mice were intraperitoneally injected one time with STZ (120 μg/g body wt) to induce partial loss of pancreatic β-cells. Three weeks after the STZ injection, the mice that exhibited hyperglycemia (over 250 mg/dl, ad libitum) were fed with HFD (D12451, 4.7 kcal/g, and 45% of energy as fat; Research Diets, New Brunswick, NJ) for 5 wk and used for the infusion experiments from 16 wk of age. The mice continued to receive HFD during the infusion and pair-feeding (PF) experiments. Age-matched male C57BL/6J mice fed SD without an STZ injection were used as normal controls (NCs).

Leptin and/or exenatide infusion experiment. The STZ/HFD mice were divided into four infusion groups [saline alone (SAL), leptin alone (LEP), exenatide alone (EX), and leptin plus exenatide (LEP/EX)] to counterbalance their starting body weights and blood glucose levels. On *day 0*, all of the mice were implanted with two miniosmotic pumps subcutaneously in the midscapular region (Alzet model 2002; Alza, Palo Alto, CA). Each pump chronically delivered either saline, recombinant mouse leptin (500 $\mu g \cdot kg^{-1} \cdot day^{-1}$; Amgen, Thousand Oaks, CA), or exenatide (20 $\mu g \cdot kg^{-1} \cdot day^{-1}$; Bachem, Bubendorf, Switzerland) for 14 days. To examine the insulinotropic effect of exenatide in NCs, we also chronically administered exenatide (20 $\mu g \cdot kg^{-1} \cdot day^{-1}$) for 14 days as described above.

Food intake and body weight. The food intake and body weight of the mice were measured every day between 1500 and 1700 for 14 days.

Indirect calorimetry. The measurement of oxygen consumption ($\dot{V}O_2$) and carbon dioxide production ($\dot{V}CO_2$) was performed 48 h between *day 9* and *10* after >72 h of acclimation using an Oxymax indirect calorimeter (Columbus Instruments, Columbus, OH). The respiratory exchange ratio [RER, ratio of CO_2 production to O_2 ($\dot{V}CO_2/\dot{V}O_2$)] was calculated and averaged across the measurement session.

Metabolic variables. Right before the infusion experiments, blood samples were obtained after 4 h of fasting. During the infusion experiments, ad libitum blood glucose levels were determined after tail bleeds using a reflectance glucometer by the glucose oxidase method between 1500 and 1700. At the end of the infusion experiment, blood was obtained from the inferior vena cava after 4 h of fasting. The plasma levels of insulin, leptin, triglyceride, total cholesterol, and nonesterified fatty acid (NEFA) were measured as described previously (20). The plasma exenatide levels were measured using ELISA kits specific for exenatide (Phoenix Pharmaceuticals, Burlingame, CA).

Insulin tolerance test and intraperitoneal glucose tolerance test. Either an insulin tolerance test (ITT) or intraperitoneal glucose tolerance test (IPGTT) was performed in each mouse on *day 11*. For ITTs, the mice were intraperitoneally injected with 0.4 mU/g human regular insulin (Humulin R; Eli Lilly Japan, Kobe, Japan) after 4 h of fasting. For IPGTTs, the mice were intraperitoneally injected with 1.0 mg/g glucose after overnight fasting. Blood samples were obtained from the tail vein at the indicated time points after insulin or glucose injection. GSIS was assessed by dividing the incremental insulin response by the incremental glucose response from 0 to 15 min [Δinsulin/Δglucose (0–15 min) (ng/ml ÷ mg/dl × 10^3)] during IPGTTs.

Pancreatic, liver, and skeletal muscle triglyceride levels and pancreatic insulin level. The pancreas, liver, and gastrocnemius muscles were isolated at the end of the experiments after 4 h of fasting. Tissue triglyceride and pancreatic insulin levels were measured as described previously (20, 28).

PF experiment. The STZ/HFD mice were randomly divided into three groups (SAL, LEP/EX, and PF) to counterbalance the starting body weights and blood glucose levels. The PF group was fed daily the same amount of HFD as that consumed by the LEP/EX group once at the end of the light phase for 14 days. Saline, leptin (500 $\mu g \cdot kg^{-1} \cdot day^{-1}$), and exenatide (20 $\mu g \cdot kg^{-1} \cdot day^{-1}$) were chronically infused in each group as described above for 14 days.

Data analyses. Data were expressed as means ± SE. In Figs. 1*A*, 1*D*, 1*E*, 1*F*, 3*A*, 3*B*, 4*C*, 4*D*, and 4*L*, comparisons were made using two-way repeated-measure ANOVA models for all the data. For within-group and between-group comparisons, corresponding contrasts were tested within the model. Between-group comparisons were made at all time points. In Table 1, comparisons were made using Student's *t*-test in each parameter. In the other figures and Table 2, comparisons were made using one-way ANOVA followed by Tukey's multiple-comparison test. A P value <0.05 was considered statistically significant.

RESULTS

Generation of the mouse model of type 2 diabetes with increased adiposity. As shown in Table 1, the STZ/HFD mice manifested hyperphagia and increased body weight. Hyperglycemia was exacerbated, although the plasma insulin levels were similar to those in NCs, suggesting the development of insulin resistance and impaired β-cell ability to secrete insulin adequately. In these mice, the plasma cholesterol and tissue triglyceride levels were also increased. Reduced pancreatic insulin levels in the STZ/HFD mice suggested substantial loss of pancreatic β-cells. GSIS was also reduced. These charac-

Table 1. *Metabolic characteristics of the mouse model of type 2 diabetes with increased adiposity*

Variables	Mouse Group	
	NC	STZ/HFD
Food intake, kcal/wk	82.1 ± 2.1	98.6 ± 3.4**
Body wt, g	25.9 ± 0.4	28.2 ± 0.5**
Leptin, ng/ml	2.4 ± 0.1	5.4 ± 0.3**
Blood glucose, mg/dl	124.9 ± 4.5	407.5 ± 30.6**
Insulin, ng/ml	0.97 ± 0.07	1.03 ± 0.06
Triglyceride, mg/dl	56.4 ± 2.4	57.3 ± 5.2
NEFA, meq/l	0.47 ± 0.03	0.56 ± 0.03
Total cholesterol, mg/dl	43.7 ± 3.8	93.6 ± 4.3**
Muscle triglyceride level, mg/g tissue	4.9 ± 1.5	11.1 ± 2.2*
Liver triglyceride level, mg/g tissue	10.0 ± 1.1	30.7 ± 3.3**
Pancreatic triglyceride level, mg/g tissue	5.7 ± 1.0	24.1 ± 5.2**
Pancreatic insulin level, ng/mg tissue	519.4 ± 22.4	28.4 ± 4.2**
GSIS [Δinsulin/Δglucose (0–15 min)], ng/ml ÷ mg/dl × 10^3	1.2 ± 0.2	−0.1 ± 0.2**
GSIS under exenatide infusion [Δinsulin/Δglucose (0–15 min)], ng/ml ÷ mg/dl × 10^3	3.2 ± 0.9	0.4 ± 0.5*

Data are reported as means ± SE. NC, normal chow; STZ, streptozotocin; HFD, high-fat diet; NEFA, nonesterified fatty acid. Parameters except for food intake, tissue triglyceride levels, pancreatic insulin levels, and glucose-stimulated insulin secretion (GSIS) were measured right before the infusion experiment. Food intake was measured during 14 days of the saline infusion and halved; tissue triglyceride levels and pancreatic insulin levels were measured after the 14 days of saline infusion (n = 8 mice in each group). GSIS and GSIS under exenatide infusion were assessed as described in detail in MATERIALS AND METHODS (n = 5–6 mice in each group). *P < 0.05 and **P < 0.01 vs. NC.

Table 2. *Plasma leptin and exenatide levels in leptin- and/or exenatide-infused STZ/HFD mice*

Variables	Infusion Group			
	SAL	LEP	EX	LEP/EX
Leptin, ng/ml	8.6 ± 1.3	38.5 ± 5.1**††	5.2 ± 0.3	24.0 ± 4.4*#††
Exenatide, pmol/l	ND	ND	286.0 ± 78.9	235.7 ± 31.4

Data are reported as means ± SE; n = 12–14 mice in each group for leptin and n = 4–5 mice in each group for exenatide. SAL, slaine alone; LEP, leptin alone; EX, exenatide alone. Plasma samples were obtained on *day 14* of the infusion experiment. *P < 0.05 and **P < 0.01 vs. SAL. #P < 0.05 vs. LEP. ††P < 0.01 vs. EX. ND, not detected.

teristics were compatible with human type 2 diabetes with increased adiposity.

Effects of leptin and/or exenatide on glucose metabolism in the STZ/HFD mice. Continuous administration of leptin (500 $\mu g \cdot kg^{-1} \cdot day^{-1}$) and exenatide (20 $\mu g \cdot kg^{-1} \cdot day^{-1}$) elevated plasma leptin levels to almost 20–30 ng/ml above baseline and plasma exenatide levels to around 250 pmol/l, respectively, in the STZ/HFD mice (Table 2).

After the infusions, LEP, EX, and LEP/EX significantly corrected hyperglycemia. Furthermore, LEP/EX corrected hyperglycemia to a greater extent than either monotherapy (Fig. 1, *A* and *B*). Plasma insulin levels were not significantly different among each infusion group and the NC group (Fig. 1*C*), suggesting that factors affecting insulin secretion, such as blood glucose and lipid levels, insulin sensitivity, and other insulin secretagogues, worked differently in each group. Following this, we performed ITT to evaluate the effects on insulin sensitivity, the results of which showed a marked decrease in blood glucose levels in the LEP/EX group than in the other groups (Fig. 1*D*). Next, we performed IPGTT to evaluate the effects on insulin secretion, the results of which showed significant improvement of glucose tolerance in the LEP/EX group than in the other three infusion groups (Fig. 1*E*). The plasma insulin levels in the SAL group at 15 min did not increase from those at 0 min (Fig. 1*F*), and Δinsulin/Δglucose (0–15 min) values were severely reduced compared with those in the NC group (Fig. 1*G*), indicating reduced GSIS in the STZ/HFD mice (Table 1). In addition, GSIS under exenatide infusion, the Δinsulin/Δglucose (0–15 min) values in the exenatide (20 $\mu g \cdot kg^{-1} \cdot day^{-1}$)-infused mice, were markedly reduced in the STZ/HFD mice compared with those in the NC group (Table 1), suggesting a reduced insulinotropic effect

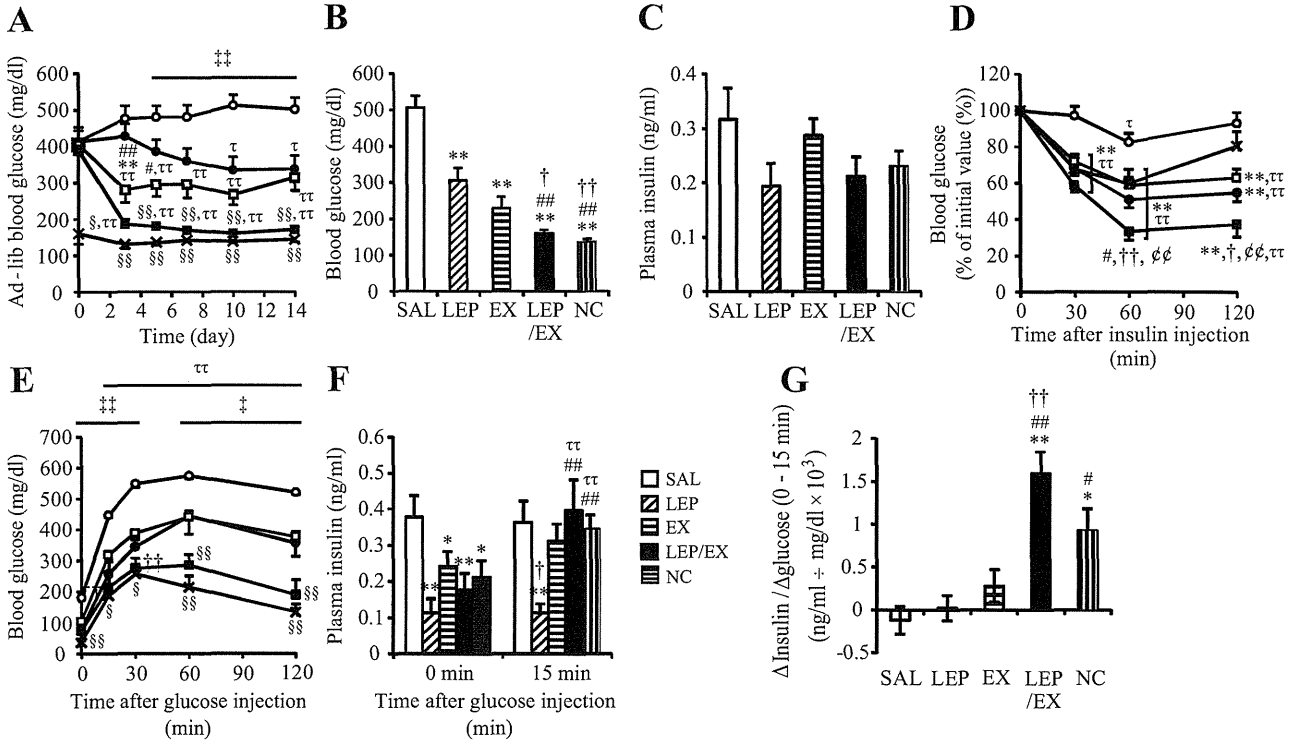

Fig. 1. Effects of leptin and/or exenatide on glucose metabolism in the streptozotocin (STZ)/high-fat diet (HFD) mice. *A*: ad libitum blood glucose levels in the saline alone (SAL, white circles), leptin alone (LEP, black circles), exenatide alone (EX, white squares), LEP/EX (black squares), and normal control (NC, cross marks) groups for 14 days (n = 14–18 mice in each infusion group; n = 8 mice in NC). *B* and *C*: plasma glucose levels (*B*) and insulin levels (*C*) on *day 14* (n = 14–18 in each group). *D*: %decrease of initial value of blood glucose levels during the insulin tolerance test (ITT) in the same four infusion groups and NC group on *day 11* (n = 8–10 in each group). *E*: blood glucose levels during the intraperitoneal glucose tolerance test (IPGTT, n = 8–10 in each group). *F*: plasma insulin levels at 0 and 15 min during IPGTT (n = 8–10 in each group). *G*: Δinsulin/Δglucose (0–15 min) values in IPGTT (n = 8–10 in each group). Data are reported as means ± SE. Between-group significant differences are indicated at each time point. *P < 0.05 and **P < 0.01 vs. SAL. #P < 0.05 and ##P < 0.01 vs. LEP. †P < 0.05 and ††P < 0.01 vs. EX. ¢¢P < 0.01 vs. NC. §P < 0.05 and §§P < 0.01 vs. SAL, LEP, and EX. ‡P < 0.05 and ‡‡P < 0.01 for SAL vs. the others. τP < 0.05 and ττP < 0.01 vs. the value at *day 0* or 0 min in the same infusion group.

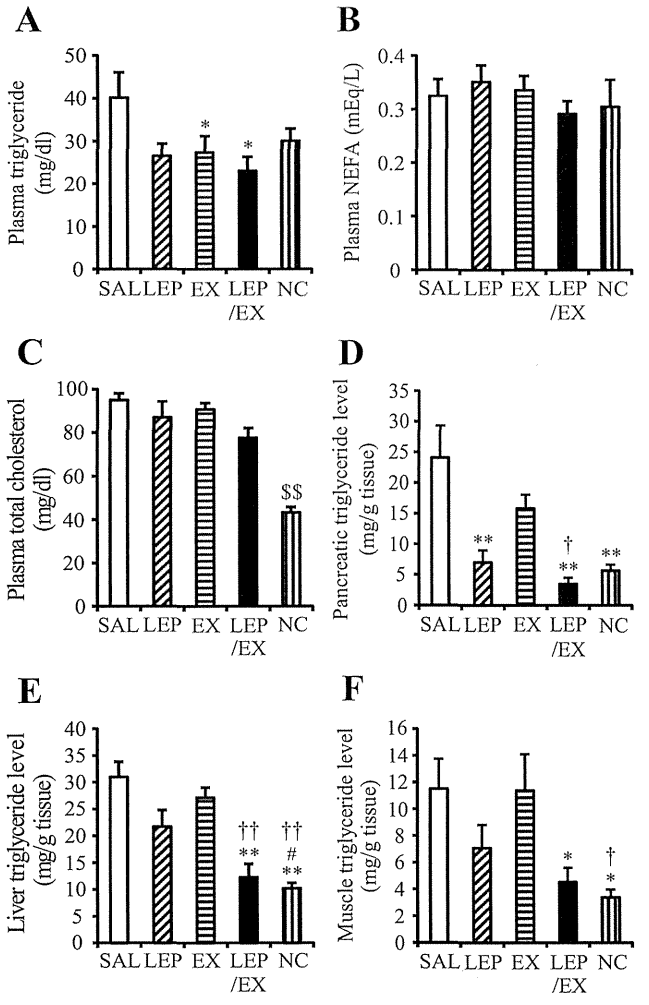

Fig. 2. Effects of leptin and/or exenatide on lipid metabolism in the STZ/HFD mice. *A–C*: plasma triglyceride (*A*), nonesterified fatty acid (NEFA, *B*), and total cholesterol (*C*) levels on *day 14* (n = 12–14 in each infusion group; n = 8 in NC). *D–F*: pancreas (n = 7–10 in each group; *D*), liver (n = 12–14 in each infusion group; n = 8 in NC; *E*), and gastrocnemius muscle (n = 8–9 in each group; *F*) triglyceride levels on *day 14*. Data are reported as means ± SE. $^{*}P < 0.05$ and $^{**}P < 0.01$ vs. SAL. $\#P < 0.05$ vs. LEP. $\dagger P < 0.05$ and $\dagger\dagger P < 0.01$ vs. EX. $\$\$P < 0.01$ for NC vs. the others.

of exenatide in the STZ/HFD mice. However, LEP/EX significantly increased plasma insulin levels at 15 min from those at 0 min (Fig. 1*F*) and markedly augmented the Δinsulin/Δglucose (0–15 min) values than the other three infusion groups (Fig. 1*G*). In IPGTT, at 0 min, the plasma glucose levels were similar among the LEP, EX, and LEP/EX groups. These results suggested that adding leptin to exenatide restored the insulinotropic effect of exenatide in the STZ/HFD mice.

Effects of leptin and/or exenatide on plasma lipid levels and tissue triglyceride levels in the STZ/HFD mice. Because both plasma lipid levels and lipid deposition in the pancreas affect GSIS (22, 41, 45, 50), we measured plasma lipid levels and triglyceride levels in the pancreas.

After the infusion experiment, EX and LEP/EX significantly reduced plasma triglyceride levels, and LEP also tended to reduce comparable to that in the EX and LEP/EX groups (Fig. 2*A*). NEFA and total cholesterol levels remained unchanged (Fig. 2, *B* and *C*). LEP and LEP/EX markedly reduced and almost normalized pancreatic triglyceride levels. Pancreatic triglyceride levels in the LEP/EX group also significantly reduced compared with those in the EX group (Fig. 2*D*). In addition, LEP/EX markedly reduced and almost normalized and LEP tended to reduce triglyceride levels in the liver and skeletal muscle (Fig. 2, *E* and *F*).

Effects of leptin and/or exenatide on food intake, body weight, and energy expenditure in the STZ/HFD mice. Body weight reduction itself may reduce pancreatic triglyceride deposition and improve β-cell function (22, 39). Thus, we examined the effects of leptin and/or exenatide on food intake and body weight in the STZ/HFD mice. Although the body weight was increased in the SAL group during the experiment period, LEP and EX significantly reduced food intake and body weight, and, furthermore, LEP/EX reduced them to a greater extent than either monotherapy (Fig. 3, *A* and *B*). $\dot{V}O_2$ tended to increase in the LEP and LEP/EX groups (Fig. 3*C*). LEP/EX significantly decreased RER, indicating increased utilization of fat as a fuel source (Fig. 3*D*).

PF experiment. Next, we performed a PF experiment to examine the effects of anorexic and weight-reducing effects by LEP/EX on pancreatic triglyceride levels and GSIS. In the PF group, we fed daily the same amount of HFD that was consumed by the LEP/EX group for 14 days to the STZ/HFD mice (Fig. 4*A*). The PF group showed a significant reduction in body

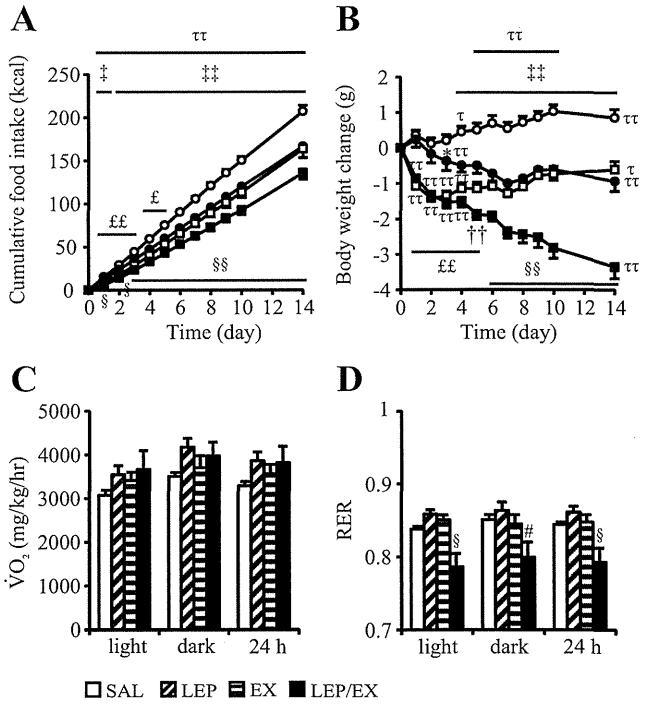

Fig. 3. Effects of leptin and/or exenatide on food intake, body weight, and energy expenditure in the STZ/HFD mice. *A* and *B*: cumulative food intake (*A*) and changes in body weight (*B*) in the SAL (white circles), LEP (black circles), EX (white squares), and LEP/EX (black squares) groups for 14 days (n = 14–18 in each group). *C* and *D*: oxygen consumption ($\dot{V}O_2$, *C*) and respiratory exchange ratio (RER, *D*) on *days 9–10* (n = 4 in each group). Data are reported as means ± SE. Between-group significant differences are indicated at each time point. $^{*}P < 0.05$ vs. SAL. $\#P < 0.05$ vs. LEP. $\dagger\dagger P < 0.01$ vs. EX. $\ddagger P < 0.05$ and $\ddagger\ddagger P < 0.01$ for SAL vs. the others. $\S P < 0.05$ and $\S\S P < 0.01$ for LEP/EX vs. SAL, LEP, and EX. $£P < 0.05$ and $££P < 0.01$ for EX and LEP/EX vs. SAL and LEP. $\tau P < 0.05$ and $\tau\tau P < 0.01$ vs. the value at *day 0* in the same infusion group.

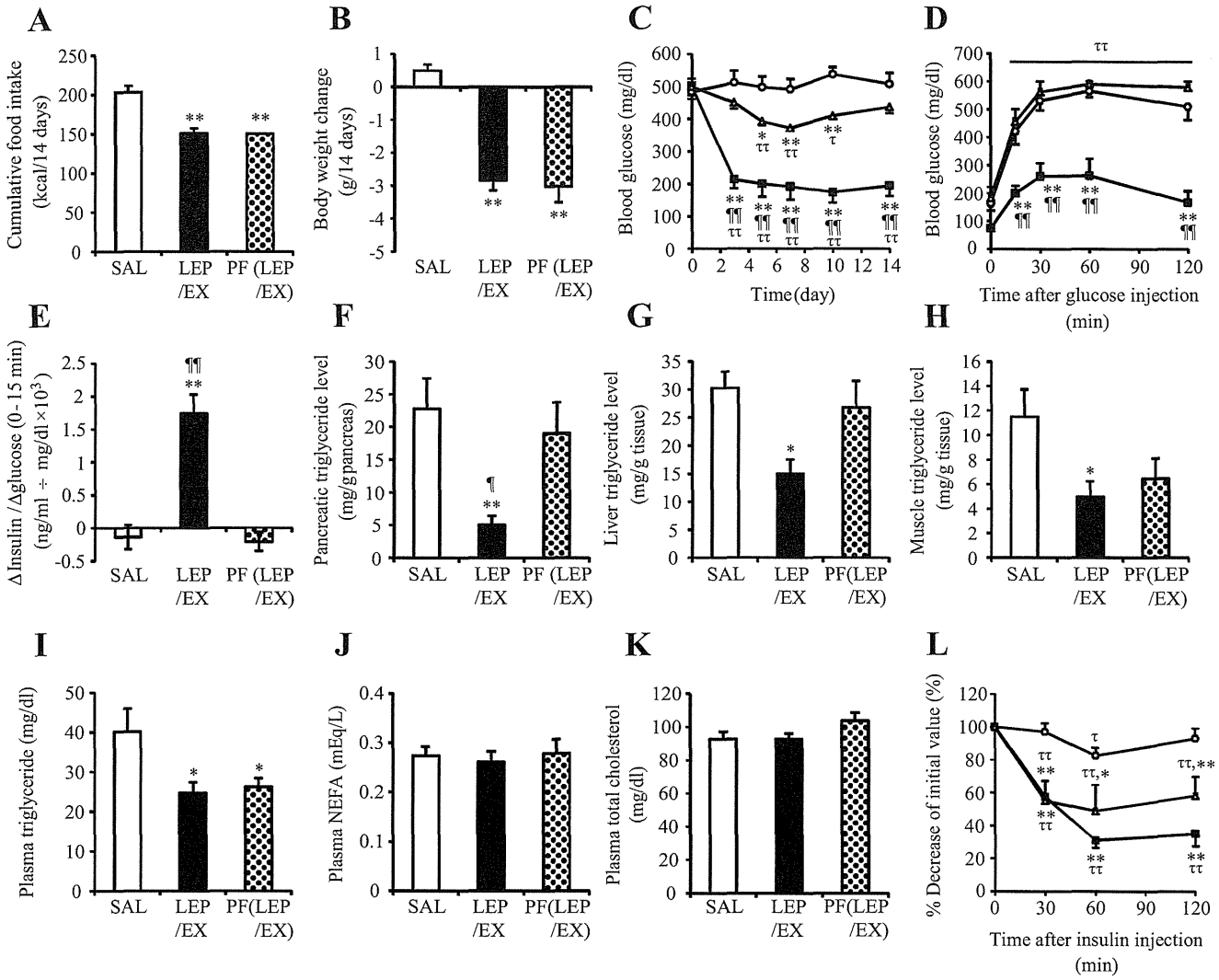

Fig. 4. Pair-feeding experiment. *A* and *B*: cumulative food intake (*A*) and changes in body weight (*B*) for 14 days (n = 11–12 in each group). *C* and *D*: ad libitum blood glucose levels for 14 days (n = 11–12 in each group; *C*) and blood glucose levels during IPGTT (n = 6–7 in each group; *D*) in the SAL (white circles), LEP/EX (black squares), and PF (white triangles) groups. *E*: Δinsulin/Δglucose (0–15 min) values in IPGTT (n = 6–8 in each group). *F–H*: pancreatic (n = 6–8 in each group; *F*), liver (n = 10–11 in each group; *G*), and skeletal muscle (n = 10–12 in each group; *H*) triglyceride levels on *day 14*. *I–K*: plasma triglyceride (*I*), NEFA (*J*), and total cholesterol (*K*) levels on *day 14* (n = 11–12 in each group). *L*: %decrease of initial value of blood glucose levels during ITT in the SAL (white circles), LEP/EX (black squares), and PF (white triangles) groups (n = 6–8 in each group). Data are reported as means ± SE. Between-group significant differences are indicated at each time point. $*P < 0.05$ and $**P < 0.01$ vs. SAL. ¶$P < 0.05$ and ¶¶$P < 0.01$ vs. PF. $\tau P < 0.05$ and $\tau\tau P < 0.01$ vs. the value at *day 0* or 0 min in the same infusion group.

weight comparable to that in the LEP/EX group (Fig. 4*B*). However, the improvement of blood glucose levels in the PF group was lower than that in the LEP/EX group (Fig. 4*C*). In IPGTT, glucose tolerance did not improve (Fig. 4*D*), and GSIS did not improve in the PF group (Fig. 4*E*). The pancreatic (Fig. 4*F*), liver (Fig. 4*G*), and skeletal muscle (Fig. 4*H*) triglyceride levels were not reduced; plasma lipid levels were comparable to those in the LEP/EX group (Fig. 4, *I*, *J*, and *K*), and the improvement of insulin sensitivity was lower in the PF group than in the LEP/EX group (Fig. 4*L*).

DISCUSSION

In the present study, we used the STZ/HFD mice as a mouse model of type 2 diabetes with increased adiposity. In the mice, adding leptin to exenatide enhanced GSIS to a greater extent than either monotherapy, which was associated with the reduction of pancreatic triglyceride levels. In addition, LEP/EX reduced tissue triglyceride levels in the liver and skeletal muscle, improved insulin sensitivity, and corrected hyperglycemia to a greater extent than either monotherapy. Furthermore, LEP/EX reduced food intake and body weight to a greater extent than either monotherapy. However, the PF experiment indicated that mechanisms other than calorie restriction were involved in the reduction of the pancreatic triglyceride level and the enhancement of GSIS by LEP/EX.

The STZ/HFD mice showed defects in the pancreatic β-cell function (Table 1 and Fig. 1, *F* and *G*) and insulin resistance (Fig. 1*D*). These characteristics are compatible with type 2 diabetes. In addition, plasma leptin levels in the mice (Table 1) suggested that they increased body weight to overweight range because it was reported that twofold increase in plasma leptin levels correspond to a body mass index in the range of 25–30

kg/m^2 in humans (33). Impaired insulin secretion due to STZ injection would have reduced the effect of HFD to increase body weight. Adiposity was also increased in the mice. Therefore, we used the STZ/HFD mice as a mouse model of type 2 diabetes with increased adiposity. Substantially reduced pancreatic insulin levels in the mice (Table 1) also suggested that they were in a late stage of type 2 diabetes. In the mice, LEP/EX markedly improved glucose metabolism.

In healthy individuals, oral glucose ingestion enhances insulin secretion to a greater extent than intravenous glucose infusion (24), which is called the "incretin effect." This effect is elicited by gut hormones such as GLP-1 and glucose-dependent insulinotropic polypeptide (GIP) called "incretin," which are released from the enteroendocrine cells of the intestine in response to meal ingestion (5, 18). However, in patients with type 2 diabetes, the insulinotropic effect of GIP is largely disappeared, and the insulinotropic effect of GLP-1 is also reduced (15, 31). Recent studies have indicated that consequences of the diabetic state, such as reduced β-cell function and mass, could largely contribute to the reduction of the incretin effect in type 2 diabetes, whereas genetic defects (i.e., allelic variation of TCF7L2 and WFS1) and reduced incretin secretion may also contribute (35, 38). Hyperglycemia and hyperlipidemia, which impair β-cell function, can also reduce the incretin effect (15, 50). In this context, Hojberg et al. recently reported that correcting hyperglycemia could restore the insulinotropic effect of GLP-1 (11), and Kang et al. also reported that correcting hyperlipidemia using bezafibrate could restore the insulinotropic effect of exenatide (14). However, in the present study, another factor, besides hyperglycemia and hyperlipidemia, was suspected to play a role in the reduction of the insulinotropic effect of exenatide. Before IPGTT, the blood glucose levels were similar among the LEP, EX, and LEP/EX groups (Fig. 1*E*). Plasma lipid levels were also similar among the three groups (Fig. 2, *A*, *B*, and *C*). However, LEP/EX enhanced GSIS to a greater extent than either monotherapy (Fig. 1*G*).

Pancreatic lipid deposition, which increases with progression of obesity, reportedly causes β-cell dysfunction (41, 45). Improvement of β-cell function associated with the reduction of pancreatic lipid deposition has been found in rodents and humans (22, 39, 46). Even in obese patients with normal glucose tolerance, the pancreatic lipid levels are increased and the incretin effect is reduced (17, 36). These reports had suggested that pancreatic lipid deposition could also affect the incretin effect; however, this has not been confirmed. In the present study, we reported for the first time the restoration of the insulinotropic effect of exenatide by the coadministration of leptin, and this effect was associated with the reduction of pancreatic triglyceride levels in the STZ/HFD mice. (Figs. 1*F*, 1*G*, and 2*D*).

Leptin itself could not be expected to produce direct insulinotropic effects; however, it may improve β-cell functions such as GSIS associated with the reduction of pancreatic lipid deposition in rodents (39, 46). This ectopic lipid-lowering effect of leptin has been reported to be far beyond its effect on food intake and body weight and was attained by mechanisms such as sympathetic nerve activation and increasing lipid oxidation (20, 25, 43). Although a GLP-1 receptor agonist could also reduce ectopic lipid deposition, a substantial effect was associated with body weight reduction (3, 40). The results of the PF experiment also suggested that the reduction of pancreatic triglyceride levels by LEP/EX was achieved by mechanisms other than weight reduction (Fig. 4). Therefore, the marked reduction of pancreatic triglyceride levels by LEP/EX (Fig. 2*D*) could have been achieved by leptin rather than exenatide, at least during the 2 wk of the experimental period. The pancreatic lipid-reducing effect of leptin may have restored β-cell function and the insulinotropic effect of exenatide in the STZ/HFD mice.

There may be some reasons that leptin alone did not restore GSIS, although it did significantly reduce the pancreatic triglyceride levels (Figs. 1*F*, 1*G*, and 2*D*). First, the intrinsic incretin levels may have not been high enough to exert the incretin effect in the LEP group. We performed IPGTT rather than an oral challenge because it enabled the investigation of insulin secretion without any confounding effects from intrinsic incretins. Therefore, incretin levels should have been low in the fasting condition of the LEP group during IPGTT. On the other hand, plasma exenatide levels in the LEP/EX group were 235.7 ± 31.4 pM (Table 2), which was comparable to the plasma GLP-1 level reported in obese patients after undergoing bariatric surgery, and could markedly improve glucose and energy metabolism (8, 21). In addition, in patients with type 2 diabetes, the physiological concentration of GLP-1 could not sufficiently induce GSIS, but a supraphysiological dose of a GLP-1 receptor agonist could; however, compared with healthy controls, the insulinotropic effect of the supraphysiological dose of GLP-1 was still reduced (15, 31). Thus the exenatide treatment may have been necessary to produce a marked restoration of GSIS by LEP/EX in the STZ/HFD mice. Second, the substantial loss of pancreatic β-cells in the STZ/HFD mice, suggested by the reduction of pancreatic insulin levels to less than 1/10th of those of the NC group (Table 1), may have masked the improvement of β-cell function with leptin. Hosokawa et al. reported that GSIS and the insulinotropic effect of GLP-1 were substantially reduced in diabetic rats after a 90% pancreatectomy (12). Thus, leptin alone could not have restored GSIS in the STZ/HFD mice.

Plasma leptin levels in the LEP group (Table 2) were comparable to the peak plasma leptin levels observed in our clinical trial of leptin replacement therapy in patients with lipodystrophy (6), and it could be clinically applicable in humans.

The anorexic and weight-reducing effects of leptin and GLP-1 are reduced in obesity (1, 4, 9, 44). However, LEP/EX enhanced these effects to a greater extent than either monotherapy (Fig. 3, *A* and *B*). These results were similar to those recent reports by Williams and others using lean and obese rodents (27, 48). As for mechanisms, Williams et al. reported that leptin could potentiate the anorexic effect of GLP-1 via central nervous system (CNS) mechanisms (48). On the other hand, the marked reduction of tissue triglyceride levels (Fig. 2, *D*, *E*, and *F*) and RER (Fig. 3*D*) by LEP/EX also suggested the action of leptin being restored because these effects were expected with leptin rather than exenatide (2, 3). GLP-1 could also regulate glucose metabolism via CNS mechanisms such as the arcuate nucleus in the hypothalamus, which plays an essential role in the glucoregulatory action of leptin (16, 37). Thus, leptin and exenatide may have interacted to restore each other's energy balance regulating and glucoregulatory effects via CNS mechanisms. This issue may also have a therapeutic

potential but requires further investigation. Furthermore, the STZ/HFD mice would not be obese but overweight as mentioned above, and the glucose-lowering effect of leptin monotherapy was partially preserved in the present study. Whether LEP/EX could exhibit marked glucose-lowering effect to a greater extent than either monotherapy even in leptin-resistant (9) obese type 2 diabetes will deserve specific attention in the future.

In conclusion, our findings suggest that leptin treatment may restore the insulinotropic effect of exenatide associated with the reduction of the pancreatic lipid deposition in type 2 diabetes with increased adiposity. In addition, the coadministration of leptin and exenatide reduced food intake and body weight to a greater extent than either monotherapy. Thus, combination therapy with leptin and exenatide could be an effective treatment for patients with type 2 diabetes with increased adiposity.

ACKNOWLEDGMENTS

We thank Mayumi Nagamoto for technical assistance and Yoko Koyama for secretarial assistance.

GRANTS

This work was supported in part by research grants from JSPS KAKENHI (Grant No. 23791054); the Ministry of Education, Culture, Sports, Science and Technology of Japan, including a Grant-in-Aid for Scientific Research on Innovative Areas (Research in a proposed research area) "Molecular Basis and Disorders of Control of Appetite and Fat Accumulation"; the Ministry of Health, Labour and Welfare of Japan; Japan Foundation for Applied Enzymology; the Takeda Medical Research Foundation; the Smoking Research Foundation; Suzuken Memorial Foundation; Novo Nordisk Insulin Research award; and Lilly Education and Research Grant Office.

DISCLOSURES

No conflicts of interest, financial or otherwise, are declared by the authors.

AUTHOR CONTRIBUTIONS

Author contributions: T.S., T.K., K.E., and K.N. conception and design of research; T.S. performed experiments; T.S. analyzed data; T.S., T.K., K.E., D.A., S.Y.-K., Z.M., V.M.J.G., C.E., M.A.-A., Y.Y., M.N., J.F., K.H., N.I., and K.N. interpreted results of experiments; T.S. prepared figures; T.S. drafted manuscript; T.S., T.K., and K.N. approved final version of manuscript; T.K., K.E., N.I., and K.N. edited and revised manuscript.

REFERENCES

1. **Aotani D, Ebihara K, Sawamoto N, Kusakabe T, Aizawa-Abe M, Kataoka S, Sakai T, Iogawa H, Ebihara C, Fujikura J, Hosoda K, Fukuyama H, Nakao K.** Functional magnetic resonance imaging analysis of food-related brain activity in patients with lipodystrophy undergoing leptin replacement therapy. *J Clin Endocrinol Metab* 97: 3663–3671, 2012.
2. **Bradley DP, Kulstad R, Racine N, Shenker Y, Meredith M, Schoeller DA.** Alterations in energy balance following exenatide administration. *Appl Physiol Nutr Metab* 37: 893–899, 2012.
3. **Cummings BP, Stanhope KL, Graham JL, Baskin DG, Griffen SC, Nilsson C, Sams A, Knudsen LB, Raun K, Havel PJ.** Chronic administration of the glucagon-like peptide-1 analog, liraglutide, delays the onset of diabetes and lowers triglycerides in UCD-T2DM rats. *Diabetes* 59: 2653–2661, 2010.
4. **Duca FA, Sakar Y, Covasa M.** Combination of obesity and high-fat feeding diminishes sensitivity to GLP-1R agonist exendin-4. *Diabetes* 62: 2410–2415, 2013.
5. **Dupre J, Ross SA, Watson D, Brown JC.** Stimulation of insulin secretion by gastric inhibitory polypeptide in man. *J Clin Endocrinol Metab* 37: 5: 826–828, 1973.
6. **Ebihara K, Kusakabe T, Hirata M, Masuzaki H, Miyanaga F, Kobayashi N, Tanaka T, Chusho H, Miyazawa T, Hayashi T, Hosoda K, Ogawa Y, DePaoli AM, Fukushima M, Nakao K.** Efficacy and safety of leptin-replacement therapy and possible mechanisms of leptin actions in patients with generalized lipodystrophy. *J Clin Endocrinol Metab* 92: 532–541, 2007.
7. **Ebihara K, Ogawa Y, Masuzaki H, Shintani M, Miyanaga F, Aizawa-Abe M, Hayashi T, Hosoda K, Inoue G, Yoshimasa Y, Gavrilova O, Reitman ML, Nakao K.** Transgenic overexpression of leptin rescues insulin resistance and diabetes in a mouse model of lipoatrophic diabetes. *Diabetes* 50: 1440–1448, 2001.
8. **Goldfine AB, Mun EC, Devine E, Bernier R, Baz-Hecht M, Jones DB, Schneider BE, Holst JJ, Patti ME.** Patients with neuroglycopenia after gastric bypass surgery have exaggerated incretin and insulin secretory responses to a mixed meal. *J Clin Endocrinol Metab* 92: 4678–4685, 2007.
9. **Heymsfield SB, Greenberg AS, Fujioka K, Dixon RM, Kushner R, Hunt T, Lubina JA, Patane J, Self B, Hunt P, McCamish M.** Recombinant leptin for weight loss in obese and lean adults: a randomized, controlled, dose-escalation trial. *J Am Med Assoc* 282: 1568–1575, 1999.
10. **Hodson DJ, Mitchell RK, Bellomo EA, Sun G, Vinet L, Meda P, Li D, Li WH, Bugliani M, Marchetti P, Bosco D, Piemonti L, Johnson P, Hughes SJ, Rutter GA.** Lipotoxicity disrupts incretin-regulated human beta cell connectivity. *J Clin Invest* 123: 4182–4194, 2013.
11. **Hojberg PV, Vilsboll T, Rabol R, Knop FK, Bache M, Krarup T, Holst JJ, Madsbad S.** Four weeks of near-normalisation of blood glucose improves the insulin response to glucagon-like peptide-1 and glucose-dependent insulinotropic polypeptide in patients with type 2 diabetes. *Diabetologia* 52: 199–207, 2009.
12. **Hosokawa YA, Hosokawa H, Chen C, Leahy JL.** Mechanism of impaired glucose-potentiated insulin secretion in diabetic 90% pancreatectomy rats. Study using glucagon-like peptide-1 (7–37). *J Clin Invest* 97: 180–186, 1996.
13. **Kamohara S, Burcelin R, Halaas JL, Friedman JM, Charron MJ.** Acute stimulation of glucose metabolism in mice by leptin treatment. *Nature* 389: 374–377, 1997.
14. **Kang ZF, Deng Y, Zhou Y, Fan RR, Chan JC, Laybutt DR, Luzuriaga J, Xu G.** Pharmacological reduction of NEFA restores the efficacy of incretin-based therapies through GLP-1 receptor signalling in the beta cell in mouse models of diabetes. *Diabetologia* 56: 423–433, 2013.
15. **Kjems LL, Holst JJ, Volund A, Madsbad S.** The influence of GLP-1 on glucose-stimulated insulin secretion: effects on beta-cell sensitivity in type 2 and nondiabetic subjects. *Diabetes* 52: 380–386, 2003.
16. **Knauf C, Cani PD, Perrin C, Iglesias MA, Maury JF, Bernard E, Benhamed F, Gremeaux T, Drucker DJ, Kahn CR, Girard J, Tanti JF, Delzenne NM, Postic C, Burcelin R.** Brain glucagon-like peptide-1 increases insulin secretion and muscle insulin resistance to favor hepatic glycogen storage. *J Clin Invest* 115: 3554–3563, 2005.
17. **Knop FK, Aaboe K, Vilsboll T, Volund A, Holst JJ, Krarup T, Madsbad S.** Impaired incretin effect and fasting hyperglucagonaemia characterizing type 2 diabetic subjects are early signs of dysmetabolism in obesity. *Diabetes Obes Metab* 14: 500–510, 2012.
18. **Kreymann B, Williams G, Ghatei MA, Bloom SR.** Glucagon-like peptide-1 7–36: a physiological incretin in man. *Lancet* 2: 8571: 1300–1304, 1987.
19. **Kusakabe T, Ebihara K, Sakai T, Miyamoto L, Aotani D, Yamamoto Y, Yamamoto-Kataoka S, Aizawa-Abe M, Fujikura J, Hosoda K, Nakao K.** Amylin improves the effect of leptin on insulin sensitivity in leptin-resistant diet-induced obese mice. *Am J Physiol Endocrinol Metab* 302: E924–E931, 2012.
20. **Kusakabe T, Tanioka H, Ebihara K, Hirata M, Miyamoto L, Miyanaga F, Hige H, Aotani D, Fujisawa T, Masuzaki H, Hosoda K, Nakao K.** Beneficial effects of leptin on glycaemic and lipid control in a mouse model of type 2 diabetes with increased adiposity induced by streptozotocin and a high-fat diet. *Diabetologia* 52: 675–683, 2009.
21. **Laferrere B, Teixeira J, McGinty J, Tran H, Egger JR, Colarusso A, Kovack B, Bawa B, Koshy N, Lee H, Yapp K, Olivan B.** Effect of weight loss by gastric bypass surgery versus hypocaloric diet on glucose and incretin levels in patients with type 2 diabetes. *J Clin Endocrinol Metab* 93: 2479–2485, 2008.
22. **Lim EL, Hollingsworth KG, Aribisala BS, Chen MJ, Mathers JC, Taylor R.** Reversal of type 2 diabetes: normalisation of beta cell function in association with decreased pancreas and liver triacylglycerol. *Diabetologia* 54: 2506–2514, 2011.
23. **Masuzaki H, Ogawa Y, Aizawa-Abe M, Hosoda K, Suga J, Ebihara K, Satoh N, Iwai H, Inoue G, Nishimura H, Yoshimasa Y, Nakao K.** Glucose metabolism and insulin sensitivity in transgenic mice overex-

pressing leptin with lethal yellow agouti mutation: usefulness of leptin for the treatment of obesity-associated diabetes. *Diabetes* 48: 1615–1622, 1999.

24. **McIntyr EN, Holdsworth CD, Turner DS.** New interpretation of oral glucose tolerance. *Lancet* 2: 20–21, 1964.
25. **Miyamoto L, Ebihara K, Kusakabe T, Aotani D, Yamamoto-Kataoka S, Sakai T, Aizawa-Abe M, Yamamoto Y, Fujikura J, Hayashi T, Hosoda K, Nakao K.** Leptin activates hepatic 5′-AMP-activated protein kinase through sympathetic nervous system and alpha1-adrenergic receptor: a potential mechanism for improvement of fatty liver in lipodystrophy by leptin. *J Biol Chem* 287: 40441–40447, 2012.
26. **Miyanaga F, Ogawa Y, Ebihara K, Hidaka S, Tanaka T, Hayashi S, Masuzaki H, Nakao K.** Leptin as an adjunct of insulin therapy in insulin-deficient diabetes. *Diabetologia* 46: 1329–1337, 2003.
27. **Muller TD, Sullivan LM, Habegger K, Yi CX, Kabra D, Grant E, Ottaway N, Krishna R, Holland J, Hembree J, Perez-Tilve D, Pfluger PT, DeGuzman MJ, Siladi ME, Kraynov VS, Axelrod DW, DiMarchi R, Pinkstaff JK, Tschop MH.** Restoration of leptin responsiveness in diet-induced obese mice using an optimized leptin analog in combination with exendin-4 or FGF21. *J Pept Sci* 18: 383–393, 2012.
28. **Naito M, Fujikura J, Ebihara K, Miyanaga F, Yokoi H, Kusakabe T, Yamamoto Y, Son C, Mukoyama M, Hosoda K, Nakao K.** Therapeutic impact of leptin on diabetes, diabetic complications, and longevity in insulin-deficient diabetic mice. *Diabetes* 60: 2265–2273, 2011.
29. **Nauck M, Stockmann F, Ebert R, Creutzfeldt W.** Reduced incretin effect in type 2 (non-insulin-dependent) diabetes. *Diabetologia* 29: 46–52, 1986.
30. **Nauck MA, El-Ouaghlidi A, Gabrys B, Hucking K, Holst JJ, Deacon CF, Gallwitz B, Schmidt WE, Meier JJ.** Secretion of incretin hormones (GIP and GLP-1) and incretin effect after oral glucose in first-degree relatives of patients with type 2 diabetes. *Regul Pept* 122: 209–217, 2004.
31. **Nauck MA, Heimesaat MM, Orskov C, Holst JJ, Ebert R, Creutzfeldt W.** Preserved incretin activity of glucagon-like peptide 1 [7–36 amide] but not of synthetic human gastric inhibitory polypeptide in patients with type-2 diabetes mellitus. *J Clin Invest* 91: 301–307, 1993.
32. **Ogawa Y, Masuzaki H, Hosoda K, Aizawa-Abe M, Suga J, Suda M, Ebihara K, Iwai H, Matsuoka N, Satoh N, Odaka H, Kasuga H, Fujisawa Y, Inoue G, Nishimura H, Yoshimasa Y, Nakao K.** Increased glucose metabolism and insulin sensitivity in transgenic skinny mice overexpressing leptin. *Diabetes* 48: 1822–1829, 1999.
33. **Peltz G, Sanderson M, Perez A, Sexton K, Ochoa Casares D, Fadden MK.** Serum leptin concentration, adiposity, and body fat distribution in Mexican-Americans. *Arch Med Res* 38: 5: 563–570, 2007.
34. **Perry RJ, Zhang XM, Zhang D, Kumashiro N, Camporez JP, Cline GW, Rothman DL, Shulman GI.** Leptin reverses diabetes by suppression of the hypothalamic-pituitary-adrenal axis. *Nat Med* 20: 7: 759–763, 2014.
35. **Pilgaard K, Jensen CB, Schou JH, Lyssenko V, Wegner L, Brons C, Vilsboll T, Hansen T, Madsbad S, Holst JJ, Volund A, Poulsen P, Groop L, Pedersen O, Vaag AA.** The T allele of rs7903146 TCF7L2 is associated with impaired insulinotropic action of incretin hormones, reduced 24 h profiles of plasma insulin and glucagon, and increased hepatic glucose production in young healthy men. *Diabetologia* 52: 1298–1307, 2009.
36. **Saisho Y, Butler AE, Meier JJ, Monchamp T, Allen-Auerbach M, Rizza RA, Butler PC.** Pancreas volumes in humans from birth to age one hundred taking into account sex, obesity, and presence of type-2 diabetes. *Clin Anat* 20: 933–942, 2007.
37. **Sandoval DA, Bagnol D, Woods SC, D'Alessio DA, Seeley RJ.** Arcuate glucagon-like peptide 1 receptors regulate glucose homeostasis but not food intake. *Diabetes* 57: 2046–2054, 2008.
38. **Schafer SA, Mussig K, Staiger H, Machicao F, Stefan N, Gallwitz B, Haring HU, Fritsche A.** A common genetic variant in WFS1 determines impaired glucagon-like peptide-1-induced insulin secretion. *Diabetologia* 52: 1075–1082, 2009.
39. **Shimabukuro M, Koyama K, Chen G, Wang MY, Trieu F, Lee Y, Newgard CB, Unger RH.** Direct antidiabetic effect of leptin through triglyceride depletion of tissues. *Proc Natl Acad Sci USA* 94: 4637–4641, 1997.
40. **Sorhede Winzell M, Ahren B.** Glucagon-like peptide-1 and islet lipolysis. *Horm Metab Res* 36: 795–803, 2004.
41. **Szczepaniak LS, Victor RG, Mathur R, Nelson MD, Szczepaniak EW, Tyer N, Chen I, Unger RH, Bergman RN, Lingvay I.** Pancreatic steatosis and its relationship to beta-cell dysfunction in humans: racial and ethnic variations. *Diabetes Care* 35: 2377–2383, 2012.
42. **Tamura Y, Tanaka Y, Sato F, Choi JB, Watada H, Niwa M, Kinoshita J, Ooka A, Kumashiro N, Igarashi Y, Kyogoku S, Maehara T, Kawasumi M, Hirose T, Kawamori R.** Effects of diet and exercise on muscle and liver intracellular lipid contents and insulin sensitivity in type 2 diabetic patients. *J Clin Endocrinol Metab* 90: 3191–3196, 2005.
43. **Tanaka T, Hidaka S, Masuzaki H, Yasue S, Minokoshi Y, Ebihara K, Chusho H, Ogawa Y, Toyoda T, Sato K, Miyanaga F, Fujimoto M, Tomita T, Kusakabe T, Kobayashi N, Tanioka H, Hayashi T, Hosoda K, Yoshimatsu H, Sakata T, Nakao K.** Skeletal muscle AMP-activated protein kinase phosphorylation parallels metabolic phenotype in leptin transgenic mice under dietary modification. *Diabetes* 54: 2365–2374, 2005.
44. **Turton MD, O'Shea D, Gunn I, Beak SA, Edwards CM, Meeran K, Choi SJ, Taylor GM, Heath MM, Lambert PD, Wilding JP, Smith DM, Ghatei MA, Herbert J, Bloom SR.** A role for glucagon-like peptide-1 in the central regulation of feeding. *Nature* 379: 69–72, 1996.
45. **Tushuizen ME, Bunck MC, Pouwels PJ, Bontemps S, van Waesberghe JH, Schindhelm RK, Mari A, Heine RJ, Diamant M.** Pancreatic fat content and beta-cell function in men with and without type 2 diabetes. *Diabetes Care* 30: 2916–2921, 2007.
46. **Wang MY, Koyama K, Shimabukuro M, Mangelsdorf D, Newgard CB, Unger RH.** Overexpression of leptin receptors in pancreatic islets of Zucker diabetic fatty rats restores GLUT-2, glucokinase, and glucose-stimulated insulin secretion. *Proc Natl Acad Sci USA* 95: 11921–11926, 1998.
47. **Wang MY, Chen L, Clark GO, Lee Y, Stevens RD, Ilkayeva OR, Wenner BR, Bain JR, Charron MJ, Newgard CB, Unger RH.** Leptin therapy in insulin-deficient type I diabetes. *Proc Natl Acad Sci USA* 107: 4813–4819, 2010.
48. **Williams DL, Baskin DG, Schwartz MW.** Leptin regulation of the anorexic response to glucagon-like peptide-1 receptor stimulation. *Diabetes* 55: 3387–3393, 2006.
49. **Xu G, Kaneto H, Laybutt DR, Duvivier-Kali VF, Trivedi N, Suzuma K, King GL, Weir GC, Bonner-Weir S.** Downregulation of GLP-1 and GIP receptor expression by hyperglycemia: possible contribution to impaired incretin effects in diabetes. *Diabetes* 56: 1551–1558, 2007.
50. **Zhou YP, Grill VE.** Long-term exposure of rat pancreatic islets to fatty acids inhibits glucose-induced insulin secretion and biosynthesis through a glucose fatty acid cycle. *J Clin Invest* 93: 870–876, 1994.

SCIENTIFIC REPORTS

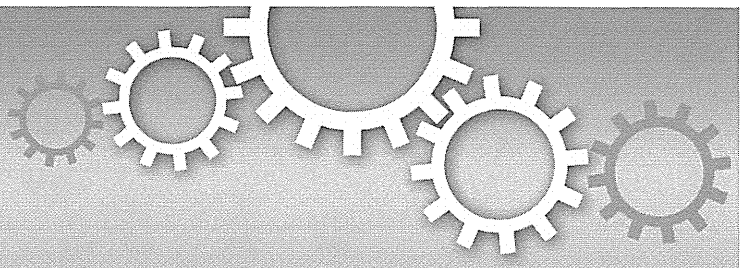

OPEN

SUBJECT AREAS:
GENE REGULATION
CARDIOMYOPATHIES
DNA RECOMBINATION
CYTOGENETICS

Received
28 August 2014

Accepted
12 December 2014

Published
16 January 2015

Correspondence and requests for materials should be addressed to T.N. (takuro-ind@umin.net)

Somatic chromosomal translocation between *Ewsr1* and *Fli1* loci leads to dilated cardiomyopathy in a mouse model

Miwa Tanaka[1], Shuichi Yamaguchi[1], Yukari Yamazaki[1], Hideyuki Kinoshita[2], Koichiro Kuwahara[2], Kazuwa Nakao[2], Patrick Y. Jay[3], Tetsuo Noda[4] & Takuro Nakamura[1]

[1]Division of Carcinogenesis, The Cancer Institute, Japanese Foundation for Cancer Research, 3-8-31 Ariake, Koto-ku, Tokyo 135-8550, Japan, [2]Department of Cardiovascular Medicine, Kyoto University Graduate School of Medicine, 54 Kawaracho Shogoin, Sakyo-ku, Kyoto 606-8507, Japan, [3]Departments of Pediatrics and Genetics, Washington University School of Medicine, 660 S Euclid Avenue, St. Louis, MO 63110, U.S.A, [4]Division of Cell Biology, The Cancer Institute, Japanese Foundation for Cancer Research, 3-8-31 Ariake, Koto-ku, Tokyo 135-8550, Japan.

A mouse model that recapitulates the human Ewing's sarcoma-specific chromosomal translocation was generated utilizing the *Cre/lox*P-mediated recombination technique. A cross between *Ewsr1-lox*P and *Fli1-lox*P mice and expression of ubiquitous Cre recombinase induced a specific translocation between *Ewsr1* and *Fli1* loci in systemic organs of both adult mice and embryos. As a result *Ewsr1-Fli1* fusion transcripts were expressed, suggesting a functional Ews-Fli1 protein might be synthesized *in vivo*. However, by two years of age, none of the *Ewsr1*-loxP/*Fli1*-loxP/CAG-Cre (EFCC) mice developed any malignancies, including Ewing-like small round cell sarcoma. Unexpectedly, all the EFCC mice suffered from dilated cardiomyopathy and died of chronic cardiac failure. Genetic recombination between *Ewsr1* and *Fli1* was confirmed in the myocardial tissue and apoptotic cell death of cardiac myocytes was observed at significantly higher frequency in EFCC mice. Moreover, expression of *Ews-Fli1* in the cultured cardiac myocytes induced apoptosis. Collectively, these results indicated that ectopic expression of the *Ews-Fli1* oncogene stimulated apoptotic signals, and suggested an important relationship between oncogenic signals and cellular context in the cell-of-origin of Ewing's sarcoma.

Chromosomal translocation is a common feature of malignant neoplasms[1]. There is growing evidence that tumor-specific translocations and inversions commonly occur among hematopoietic, mesenchymal and epithelial tumors. An increasing number of gene fusions resulting from translocation have been observed as novel technological tools have been applied. Tumor-associated chromosomal translocations include two major molecular mechanisms. One is an oncogene juxtaposition to the enhancing elements of immunoglobulin or T-cell receptor associated with lymphoid neoplasms. As a result of the juxtaposition, constitutive expression of oncogenes such as *c-MYC, BCL2* or *CCND1* induces abnormal cellular functions, including cell cycle progression and apoptosis suppression[1]. Another important outcome of translocation in cancer is gene fusion or formation of chimeric genes. Two major functional aberrations of fusion gene products are constitutive activation of signal transduction and dysregulation of transcription. Most oncogenic gene fusions in human bone and soft tissue sarcomas belong to the latter group, and there is a specific relationship between tumor types and each gene fusion[2].

To clarify the functional roles of sarcoma-specific chromosomal translocations and gene fusions, it would be ideal to induce chromosomal translocation in animal models *in vivo*. In contrast to transgenic expression of fusion genes, translocation-mediated gene fusion recapitulates gene expression levels equivalent to, and splice variants similar to those in human tumors. Inducible, site-specific chromosomal translocation has been achieved using Cre-*lox*P-mediated recombination in murine ES cells. Using this strategy, translocations between c-myc and immunoglobulin heavy chain loci, and between *Dek* and *Can* loci were successfully induced, though the efficiencies were not very high[3,4]. Indeed, a mouse model of Cre-*lox*P-mediated *in vivo* gene fusion between *Mll* and *Af9* developed acute myeloid leukemia[5]. However, it is not known whether solid tumor-related translocation *in vivo* can induce malignancies of the anticipated phenotypes.

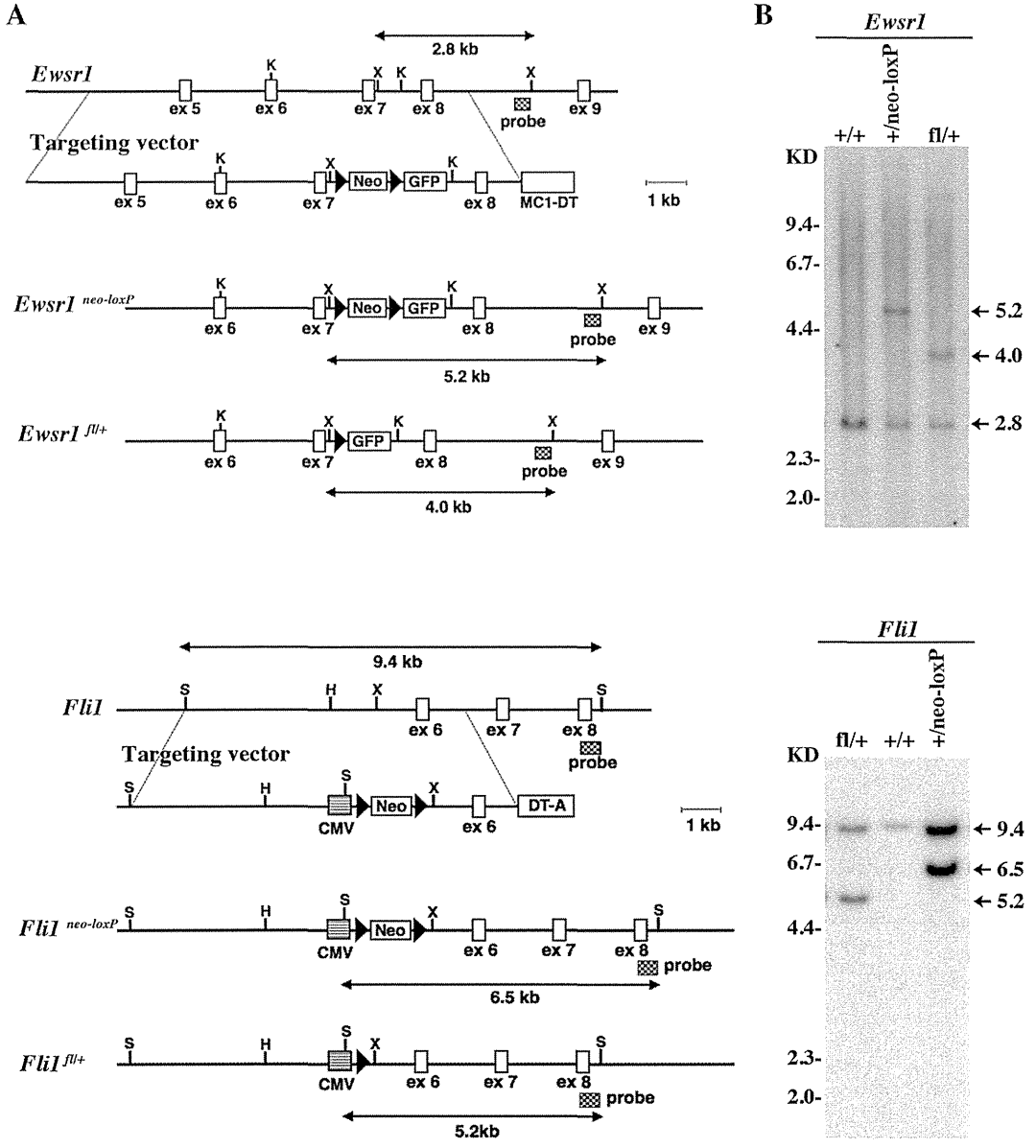

Figure 1 | Gene targeting for the *Ewsr1-Fli1* translocation model. (A) Physical maps of targeting alleles for *Ewsr1* (top) and *Fli1* (bottom) loci. Closed triangles indicate the *lox*P sequence. K: *Kpn*I, X: *Xba*I, S: *Sac*I, H: *Hin*dIII. (B) Southern blot analysis of ES cells. A 5.2 kb *Neo*-positive band and a 4.0 kb *Neo*-deleted band indicate homologous recombination of the *Ewsr1* locus as shown by *Xba*I digestion (top). A 6.5 kb *Neo*-positive band and a 5.2 kb *Neo*-deleted bands for the *Fli1* locus are shown by *Sac*I digestion (bottom). Rearranged bands are indicated by arrows.

The ETS family of transcription factors includes FLI1 and ERG. They are major fusion partners for the *EWSR1* gene in human Ewing's sarcoma[6,7]. EWS-FLI1 and EWS-ERG function as oncogenic transcription factors that dysregulate their downstream targets such as *NKX2-2*, *NR0B1* and *EZH2*[8]. It is, however, difficult to generate a good animal model by introduction of *EWS-FLI1* or *EWS-ERG* into ES cells or mouse eggs[8]. Moreover, conditional *EWS-FLI1* expression in hematopoietic cells induced myeloid and erythroid leukemia in mice[9]. Thus, it might be necessary to activate multiple target genes without activating pro-apoptosis signals for tumorigenic activity of EWS-ETS. We therefore hypothesized that EWS-ETS translocation is achieved by chance in human somatic cells of appropriate lineages and differentiation status, and such *in vivo* translocation could properly induce Ewing's sarcoma.

In an effort to induce Ewing's sarcoma in a mouse model, we have succeeded in promoting *in vivo* Cre-*lox*P-mediated translocation between *Ewsr1* and *Fli1* loci on chromosomes 11 and 9, respectively. Although the *Ewsr1-Fli1* fusion was confirmed at both DNA and RNA levels, no neoplastic lesion was induced in the model. Unexpectedly, the mice with systemic translocation developed dilated cardiomyopathy due to degeneration and apoptotic cell death of cardiac myocytes. The result indicates that ectopic chromosomal translocation and gene fusion activates apoptotic signals, resulting in degenerative cardiac disease.

Results

Generation of a mouse model for somatic chromosomal translocation between *Ewsr1* and *Fli1*. To induce locus-specific chromosomal translocation, *lox*P sequences were introduced into *Ewsr1* intron 7 on mouse chromosome 11 and *Fli1* intron 5 on chromosome 9 (Fig. 1A), since chromosomal breakpoints in human Ewing's sarcoma are most frequently observed in these loci[10]. Successful

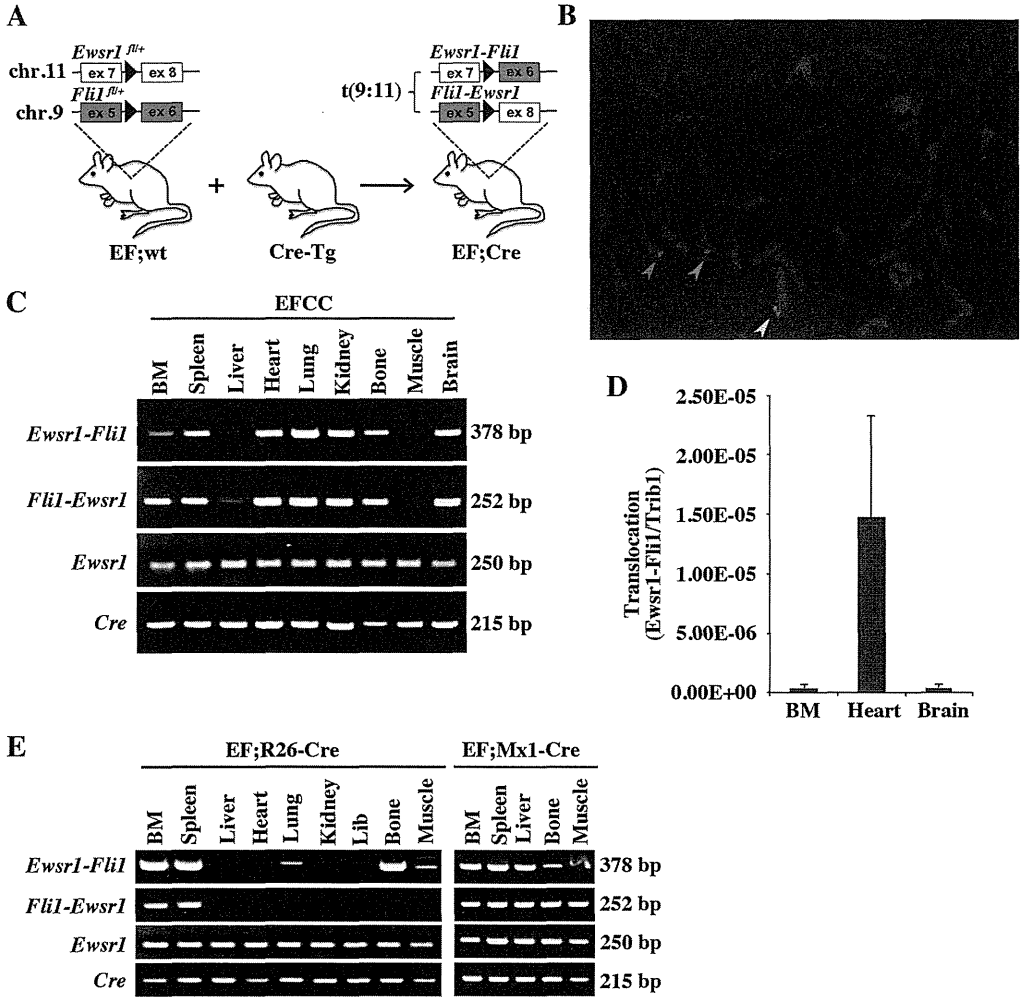

Figure 2 | Somatic chromosomal translocation between mouse chromosomes 9 and 11. (A) A schematic diagram of the *Cre*-mediated translocation model. EF;wt, *Ewsr1*$^{fl/+}$:*Fli1*$^{fl/+}$:wild-type. Cre-Tg, *Cre* transgenic. EF;Cre, *Ewsr1*$^{fl/+}$:*Fli1*$^{fl/+}$: *Cre* transgenic. Illustration of mice was drawn using Microsoft PowerPoint 2011 and then converted to tif format using Adobe Photoshop CS5. (B) Metaphase FISH shows t(9;11) translocation at *Ewsr1* and *Fli1* loci. The green fluorescence of 64E17 shows *Ewsr1* on chromosome 11 and the red fluorescence of 218O21 shows *Fli1* on chromosome 9. The yellow signal indicates translocation between two loci on *der9*. (C) The reciprocal t(9;11) translocation was shown in systemic organs of the EFCC mouse detected as *Ewsr1-Fli1* and *Fli1-Ewsr1* PCR products. *Ewsr1* amplification is shown as a loading control. (D) Estimated frequencies of translocation in bone marrow (BM), heart and brain calculated from the result of quantitative genomic PCR data in three independent mouse samples. (E) The reciprocal t(9;11) translocation in the organs of *Rosa26-CreER* and *Mx1-Cre* background detected by nested genomic PCR. Gel image shown is cropped and representative of gels run under the same experimental conditions.

knock-in of *lox*P sequences mediated by homologous recombination was confirmed for both loci in independent ES cells by Southern blotting (Fig. 1B). Both *Ewsr1*$^{fl/+}$ and *Fli1*$^{fl/+}$ mice appeared normal and healthy at birth. Germline transmission of the targeted alleles was confirmed. *Ewsr1*$^{fl/+}$ and *Fli1*$^{fl/+}$ mice were crossed to obtain mice having both mutations.

Genomic chromosomal translocation between chromosomes 9 and 11 in the *Ewsr1*$^{fl/+}$:*Fli1*$^{fl/+}$:*CAG-Cre* (EFCC) mice. The *Ewsr1*$^{fl/+}$ and *Fli1*$^{fl/+}$ mice were further crossed with *CAG-Cre*, *Mx1-Cre* or *Rosa26-CreER* mice to induce somatic chromosomal translocation between chromosomes 9 and 11 (Fig. 2A). Dual color fluorescence *in situ* hybridization (FISH) analysis of embryonic fibroblasts derived from the EFCC mice showed juxtaposition of the signal on *der9* of BAC clone RPCI-23 64E17 from chromosome 11 and that of 218O31 from chromosome 9 (Fig. 2B). Reciprocal genomic translocations in systemic organs were examined by genomic PCR using *Ewsr1*- and *Fli1*-specific primers, and both *Ewsr1-Fli1* and *Fli1-Ewsr1* translocations were detected in tail skin of all the mice examined (n = 30). The translocations in systemic organs were examined in three mice, and both *Ewsr1-Fli1* and *Fli1-Ewsr1* translocations were detected in all the organs examined (Fig. 2C). The results indicated that *lox*P-mediated recombination was effective at inducing somatic translocation by ubiquitous *Cre* recombinase expression. The frequencies of the chromosomal translocations were 1.5×10^{-5} at the highest in heart and 1×10^{-6} in bone marrow as estimated by quantitative genomic PCR comparing *Ewsr1-Fli1* and *Trib1* signals (Fig. 2D). The estimated translocation frequencies in the model are higher than those observed in ES cells described in the previous report[3]. When *Cre* recombinase was inducibly expressed by tamoxifen or polyIpolyC administration in a *Rosa26-CreER* or *Mx1-Cre* background, respectively, both *Ewsr1-Fli1* and *Fli1-Ewsr1* translocations were observed (four mice each) (Fig. 2e). However, the translocations

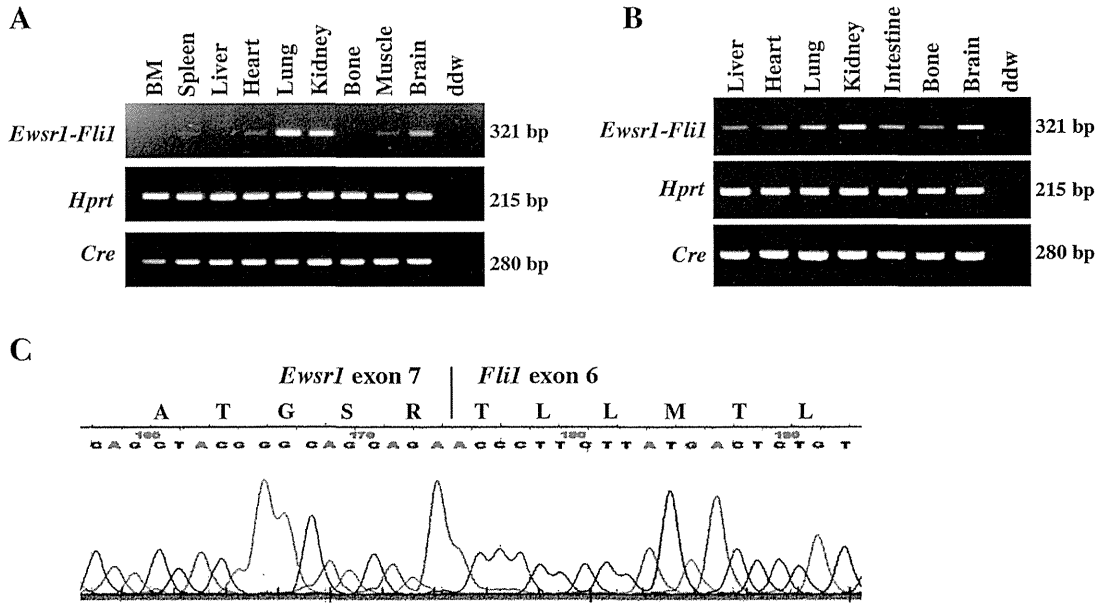

Figure 3 | *Ewsr1* is fused in-frame to *Fli1*. (A, B) RT-PCR to detect *Ews-Fli1* fusion transcripts in adult (A) and embryonic tissues (B). Data are representatives of three independent experiments with similar results. (C) Sequence analysis of the RT-PCR product using heart cDNA shows the in-frame fusion between *Ewsr1* exon 7 and *Fli1* exon 6. Deduced amino acid sequences are indicated on the nucleotide sequences.

were detected only by nested PCR in limited organs, indicating that recombination was less frequent in these *Cre* transgenes. In addition, inducible expression of *Cre* upon in the *Mx1-Cre* background resulted in translocations being limited to hematopoietic tissues.

Detection of chimeric *Ewsr1-Fli1* fusion transcripts in EFCC mice. To confirm that gene fusion between *Ewsr1* and *Fli1* was accompanied by the anticipated transcription, RT-PCR was performed using RNA samples obtained from systemic organs of both adult and embryonic mice (three mice each) (Fig. 3A, 3B). The *Ewsr1-Fli1* fusion was detected in all the embryonic organs examined, and the expression of the fusion gene was decreased in bone and liver of the adult mice. Diminished *Ewsr1-Fli1* expression in adult bone and liver might be related to decreased proliferative activity of osteochondrogenic tissues and disappearance of embryonic hematopoietic cells, respectively. No reciprocal *Fli1-Ewsr1* fusion transcript was detected in any of the organs examined (data not shown). The cDNA sequence of the *Ewsr1-Fli1* fusion transcript was analyzed by sequencing, and in-frame fusion between *Ewsr1* exon 7 and *Fli1* exon 6 was confirmed (Fig. 3C). It is expected that the fusion product included both the EWS Q-rich repeats and the FLI1 ETS DNA binding domain[11]. Thus, the data strongly suggested that a functional EWS-FLI1 protein was produced by somatic chromosomal translocation in the model.

EFCC mice died of chronic cardiac failure due to dilated cardiomyopathy. No malignant neoplasms, including Ewing's sarcoma-like lesions, were observed in EFCC mice (n = 30) for a two year period after birth. Neither sarcomas nor benign neoplasms were detect by careful examination of mice irrespective of age. Instead, most of the EFCC mice showed growth retardation and decreased motility. All the EFCC mice died by 100 weeks of age with a mean survival time of only 40 weeks (Fig. 4A). The diseased mice were carefully examined at autopsy and they showed extensive dilatation of heart (Fig. 4B). The heart weight/body weight ratio as well as heart weight itself of EFCC mice was significantly greater than that of control mice from 31 to 42 weeks (Fig 4C, Table 1). Mice of the age were selected since the severity of cardiac lesions was significantly varied in younger EFCC mice. The pathological examination further revealed the cardiac lesions and subsequent systemic congestive changes. The hearts of EFCC mice showed extensive dilatation of both the ventricles and thin ventricular wall without any signs of cardiac hypertrophy (Fig 4D). The earlier the mice became sick, the more severe the cardiac lesions were. High power views of cardiac sections indicated a disorganized arrangement of myocardial fibers with increased collagen fibers between the muscle bundles. The subendocardial area was severely affected and leukocytic infiltration was sometimes present. There was severe chronic congestion in systemic organs such as lung, liver or spleen accompanied by ischemic necrosis around the central vein of the liver (Fig. 4E).

Consistent with the pathological findings, echocardiographic analysis revealed reduced wall thickness, significant fractional shortening and decreased ejection fraction in EFCC mice (Fig. 5, Table 2). In contrast, there was no significant difference in blood pressure, heart rate or diastolic dimension between EFCC and wild-type mice (Table 2). Collectively, these findings are consistent with those of dilated cardiomyopathy.

***Ewsr1-Fli1* translocation and *Ewsr1-Fli1* expression induced myocardial damage.** To obtain insights into the mechanisms of dilated cardiomyopathy in EFCC mice, the cardiac lesion was further investigated. Laser microdissection followed by genomic PCR to detect the *Ewsr1-Fli1* translocation was carried out (Fig. 6A). *Ewsr1-Fli1* was abundantly observed in the outer area of the ventricular wall, however, no signal was detected in the subendocardial area where the myocardial damage was more severe (Fig. 6A, 1 and 3). Severer damages in the subendocardial area were observed in most of mice, though the reason for such uneven distribution of cardiac lesions was unclear. The results suggested degeneration of cardiac myocytes with translocation and perhaps gradual loss due to the pathologic effects of *Ewsr1-Fli1* expression. Indeed, a TUNEL assay using the cardiac sections showed significantly increased apoptosis in EFCC mice compared to wild-type (Fig. 6B).

The toxic effect of *Ewsr1-Fli1* was directly evaluated by its exogenous expression in cultured cardiac myocytes. The murine neonatal cardiac myocytes were infected with *Ewsr1-Fli1*-lentivirus and the frequencies of apoptosis were evaluated (Fig. 6C). The TUNEL assay

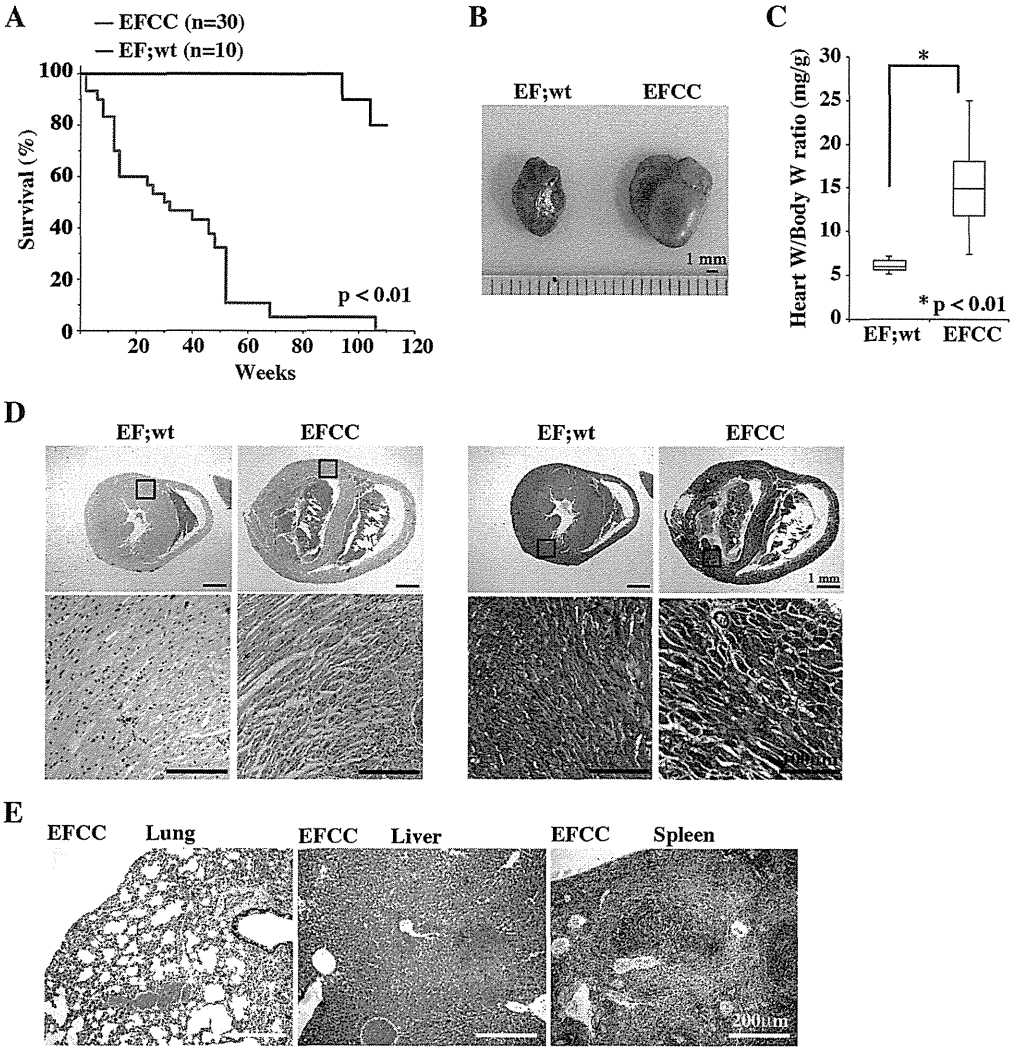

Figure 4 | EFCC mice died of chronic cardiac failure. (A) Kaplan-Meier survival curve. Statistical significance was evaluated by the log-rank test. (B) Cardiac enlargement in the EFCC mouse (right) compared to EF;wild-type (left). (C) Box plot of the heart weight/body weight ratios for EF;wild-type (n = 6) and EFCC mice (n = 6). (D) Extensive ventricular dilatation of the heart in the EFCC mouse without myocardial hypertrophy (top). High power view of myocardium with H&E (middle) and Masson's trichrome staining (bottom). Extensive fibrosis is indicated as blue staining in the EFCC heart. (E) Chronic congestion of systemic organs in EFCC mice including lung, liver and spleen. Note necrotic changes around the central vein of liver.

showed that apoptosis of cardiac myocytes was significantly increased when *Ewsr1-Fli1* was expressed in the cardiac myocytes. The Annexin V/PI flow cytometry analysis showed increases of both early and late apoptosis as well as necrosis in cardiac myocytes by *Ewsr1-Fli1* expression (Fig. 6C). These results indicated that *Ewsr1-Fli1* induced cellular apoptosis in the cardiac tissue, resulting in cellular damage and eventual dilated cardiomyopathy. In addition, *Ewsr1-Fli1* expression in human cardiac fibroblasts induced increased expression of *COL1A1* (Fig. 6D), suggesting that *Ewsr1-Fli1* may also play some role in cardiac fibrosis.

A previous study indicated that the high level of expression of Cre recombinase itself showed cardiac toxicity[12]. The expression level of the Cre protein in the hearts of the EFCC mouse was therefore compared with high-expressing *Cre* transgenic mice (Fig. 6E). *Cre* expression of EFCC mice was comparable to the low *Cre* transgenic mice that did not show cardiac lesions. The results indicated that the cardiac lesion was caused not by *Cre* expression but by *Ewsr1-Fli1*.

Discussion

Cre/*lox*P-mediated chromosomal translocations in mouse models have been reported[5,13,14]. In those studies *lox*P sites were inserted into the introns of *Mll* or *Af9* genes, and the mice carrying the mutations were crossed to place *lox*P sites in both genes. Both ubiquitous and hematopoietic-specific expression of Cre recombinase induced *in vivo* chromosomal translocation and the fusion of *Mll* and *Af9*, resulting in leukemia development. In contrast, leukemia was not observed in the mice bearing chromosomal translocation between *AML1* and *ETO in vivo* using a similar protocol[15].

In the present study, *Ewsr1-Fli1* fusion was successfully induced in various organs. Ewing's sarcoma, however, did not develop in the mice, suggesting that the cell-of-origin of Ewing's sarcoma might constitute a rare cellular population unlike hematopoietic neoplasms. Supporting this idea, we have recently succeeded in developing Ewing's sarcoma-like small round cell tumors by introducing *Ews-Fli1* or *Ews-Erg* into eSZ cells that are enriched in embryonic chondrogenic progenitors[16]. Therefore, when chromosomal translocation between *Ewsr1* and *Fli1* is efficiently induced in eSZ cells, Ewing's sarcoma can develop in a certain cohort using the current translocation model. It is likely that ubiquitous *Cre* expression affects most cell lineages both in developing and adult mouse tissues including the true cell-of-origin of Ewing's sarcoma. However, the low frequency of chromosomal recombination could